

**BIOPHYSICAL AND ECONOMIC ANALYSIS OF BLACK SPRUCE
REGENERATION IN EASTERN CANADA USING GLOBAL CLIMATE
MODEL PRODUCTIVITY OUTPUTS**

By

Jung Kuk Lee, B.Sc.

A Thesis Submitted to the School of Graduate Studies in Partial Fulfilment of the
Requirements for the Degree Master of Science

McMaster University © Copyright by Jung Lee, May 2016

MASTER OF SCIENCE (2016)
(EARTH SCIENCES)

MCMASTER UNIVERSITY
HAMILTON, ON

TITLE: Biophysical and economic analysis of Black Spruce regeneration in Eastern Canada using Global Climate Model productivity outputs

AUTHOR: Jung Lee, B.Sc. (McMaster University)

SUPERVISOR: Dr. M. Altaf Arain

NUMBER OF PAGES: ix, 58

ABSTRACT

This study explores the biophysical potential and economic attractiveness of black spruce (*Picea mariana*) regeneration in eastern Canada under future climate changes. It integrates process-based ecosystem model simulated forest productivities from three major global climate models (GCMs), growth and yield formulations specific to black spruce and economic analyses to determine the overall investment value of black spruce, both including and excluding carbon sequestration benefits. Net present value (NPV) was estimated to represent the financial attractiveness of long-rotation forest plantations through time. It was assumed that stands would not be harvested at volumes less than 80 m³ ha⁻¹. The price of stumpage was set to \$20 m⁻³, stand establishment cost was set to \$500 ha⁻¹, and the discount rate was considered at 4%, with sensitivity analyses conducted around these assumptions. The growth and yield of black spruce was simulated for an extreme future climate scenario – IPCC-RCP 8.5. The results suggested a general North-South gradient in forest productivity where gross merchantable wood volumes increased with decreasing latitudes. This pattern was also observed in NPVs, with higher values projected for the southern portion of the study area. Based on the base economic assumptions and sensitivity analyses, study results suggested that black spruce plantations are not economically attractive, unless carbon sequestration benefits of at least \$5 ton⁻¹ CO₂ are realized. Further sensitivity analyses showed that discount rate plays a significant role in determining the optimal harvest age and value. Furthermore, the optimal harvest rotation age increases with increasing carbon price by approximately 9 to 18 years.

ACKNOWLEDGEMENTS

I would like to first thank my supervisor, Dr. Altaf Arain, for the support, patience, and resources to complete my Masters and explore myself as a researcher and scholar. I am grateful for the platforms he has provided to continue my journey in research. I would also like to thank Daniel McKenney and John Pedlar. They have been a constant support and engagement to produce the finest work possible.

To the entire members of the Hydrometeorology and Climatology Research Group, words cannot describe how much I enjoyed spending my time with you guys in the office. I thank Suo Huang for her technical expertise and support for this research. Thank you to Myroslava Khomik for bringing enthusiasm and dedication to our lab. Felix, Katey, Shawn, Eric, Brandon, and Olivier, thank you for always being around for advice or a laugh.

Special thanks to my family and friends. This research simply would not be possible without their love and support.

TABLE OF CONTENTS

TITLE PAGE.....	I
DESCRIPTIVE NOTE.....	II
ABSTRACT.....	III
ACKNOWLEDGEMENTS.....	IV
LIST OF FIGURES.....	VI
LIST OF TABLES.....	VIII
SYMBOLS AND ABBREVIATIONS.....	IX
CHAPTER 1: INTRODUCTION.....	1
CHAPTER 2: DATA AND METHODS.....	6
2.1 Overview.....	6
2.2 GCM Simulated NPP.....	7
2.3 Growth and Yield estimates and NPP adjustments.....	10
2.4 Harvest Models and Economic Calculations.....	13
2.4.1 Faustmann Model.....	14
2.4.2 Incorporating Carbon Sequestration Value.....	16
2.5 Sensitivity Analysis.....	18
CHAPTER 3: RESULTS AND DISCUSSION.....	18
3.1 NPP and Growth Projection.....	18
3.2 Economic Benefits.....	22
3.3 Sensitivity Analyses.....	25
3.4 Study Significance and Future Directions.....	27
CHAPTER 4: SUMMARY AND CONCLUSIONS.....	30
REFERENCES.....	33
FIGURES.....	43
APPENDIX.....	54

LIST OF FIGURES

- Figure 1. Overview of study methodology including the integration of biogeophysical, forest growth and yield, and economic models to project future timber growth and present value estimates. We used temporal and spatial distributions of GCM-simulated NPP to modify gross merchantable volume trajectories obtained from the black spruce growth and yield model. Then, net present values were calculated with and without carbon sequestration benefits to represent the economic feasibility of the silvicultural investment using Hartman and Faustmann economic models, respectively 43
- Figure 2. Study area, focused on the province of Ontario in Canada below 52° latitude. Model grids are based on the resolutions of global climate model, GCMs (a) CanESM2 and MIROC (~2.8°) and (b) MPI (~2.5°). Study area has been divided into three regions – northwest, northeast, and southern Ontario. (a) CanESM2 and MIROC, -87.4 decimal degrees longitude is used for a division between NW and NE Ontario and 47.4 decimal degrees latitude is used for a division between northern and southern Ontario. (b) MPI, -86.4 decimal degrees longitude is used for a division between NW and NE Ontario and 48.4 decimal degrees latitude is used for a division between northern and southern Ontario 44
- Figure 3. First order condition for optimization for harvest age. The curve line is the relative value growth rate. The horizontal line represents a discount rate of 5%. The intersection of the two represents the optimal harvest age, 29.3 years, in this example 45
- Figure 4. Time series of grid-level simulated Net Primary Production (NPP) from three global climate models – (a) CanESM2 (Canadian), (b) MIROC (Japanese), and (c) MPI (European) for RCP 8.5 future climate scenario. Each line represents a grid-specific NPP estimate from 2006 to 2100. 46
- Figure 5. Spatial distribution of annual Net Primary Production (NPP) change over time in the study area as simulated by (a) CanESM2, (b) MIROC, and (c) MPI models 47

Figure 6.	Spatial distribution of gross merchantable wood volume ($\text{m}^3 \text{ha}^{-1}$) of black spruce over the study period based on (a) CanESM2-, (b) MIROC-, and (c) MPI-model simulated annual Net Primary Production (NPP) ratio, and temperature and precipitation-specific grid conditions	48
Figure 7.	Spatial distribution of NPVs of black spruce exclusive carbon sequestration benefits in the study area using Faustmann model based on (a) CanESM2, (b) MIROC, and (c) MPI models	49
Figure 8.	Spatial distribution of NPVs of black spruce inclusive of carbon sequestration benefits in the study area using a modified Hartman model based on a (a) CanESM2, (b) MIROC, and (c) MPI model	50

LIST OF TABLES

Table 1.	General assumptions and data used in baseline scenarios and sensitivity analyses	51
Table 2.	Summary table of net present values (NPVs) of timber and carbon by regions	51
Table 3.	Sensitivity analyses of wood-only scenario (Faustmann model). Optimal net present value with varying discount rate, establishment cost, and stumpage value	52
Table 4.	Sensitivity analyses of wood + carbon scenario (modified Hartman model). Optimal net present value with varying discount rate, establishment cost, stumpage value, and carbon price when the carbon uptake value is considered.	53

SYMBOLS AND ABBREVIATIONS

C	Carbon	
CO ₂	Carbon dioxide	
ESM	Earth system model	
GCM	Global climate model	
GHG	Greenhouse gas	
GPP	Gross Primary Production	(g C m ⁻² year ⁻¹)
IPCC	Intergovernmental Panel on Climate Change	
r	Discount rate	(%)
MAT	Mean annual temperature	(°C)
NEP	Net Ecosystem Production	(g C m ⁻² year ⁻¹)
NEE	Net Ecosystem Exchange	(g C m ⁻² year ⁻¹)
NPP	Net Primary Production	(g C m ⁻² year ⁻¹)
NPV	Net present value	(\$ ha ⁻¹)
OMNR	Ontario Ministry of Natural Resources	
P	Standing timber value	(\$ m ⁻³)
PREC	Annual mean precipitation	(mm)
R _a	Autotrophic respiration	
R _h	Heterotrophic respiration	
RCP	Representative concentration pathway	
RVGR	Relative value growth rate	
V	Yield volume	(m ³ ha ⁻¹)

CHAPTER 1: INTRODUCTION

Forests cover approximately 4 billion hectares (ha), which is equivalent to 30% of the Earth's land surface area, and are expected to be impacted by future climate changes (Kirilenko and Sedjo, 2007). Approximately 3.5 billion m³ of wood is harvested each year from forests globally, half of which is used as fuel (FAO, 2005). In North America, forests cover approximately 500 million ha, of which 384 million ha are located in Canada (FAO, 2010; State of Canada's Forests, 2015). Approximately 6.1 million ha of forest are harvested each year in North America, while another 1 million ha are converted to other land uses (Masek et al., 2011). Forests are recognized as significant carbon sinks, though the extent to which they function in this role is largely dependent on growth and disturbance (e.g., harvesting, fire, etc.) rates (Meinshausen *et al.*, 2009; Beer et al., 2010; Meinshausen *et al.*, 2011). Thus the stakes are high to better understand responses of forests to global change pressures, from both wood production and carbon sequestration perspectives.

In Canada, the majority (67.8%) of forests are coniferous species, with Black spruce (*Picea mariana*) being the most abundant and widely distributed species (Mann et al., 2013; Environment Canada, 2014). In Ontario, Black spruce covers approximately 17.5 million ha, which is about 41% of the province's total forest area from approximately northern limits of the Great Lakes to Hudson Bay (Haavisto and Jeglum, 1995). Black spruce is a highly adaptable species that can grow well under a range of moisture and soil conditions (Bigras and Bertrand, 2006) and can reach heights of 20 – 30 m under very

favorable site conditions. It has a high shade tolerance and can have a lifespan of about 200 years (Rossi et al., 2010). Black spruce carries important economic value as it is harvested for many different uses, such as pulp, paper, lumber, fuel wood, and Christmas trees. In Ontario alone, black spruce accounts for 80% of the annual allowable forest cut (Natural Resources Canada, 2000). This economic importance deserves attention in the context of climate change, which is expected to be a major factor shaping future boreal forest landscapes (Haavisto and Jeglum, 1995; IPCC, 2014; Bigras and Bertrand, 2006; Gauthier et al., 2015).

One potential option to help mitigate future climate change impacts is to use forest ecosystems to sequester atmospheric carbon dioxide (CO₂) (van Kooten *et al.*, 1999). These efforts may include both reforestation and afforestation. Reforestation is the re-establishment of forest tree species by natural regeneration or artificial means (e.g. planting seedlings) and the harvest of a stand. Afforestation is the establishment of a new forest in areas where no forests have grown for at least 50 years (van Kooten *et al.*, 1999; McKenney *et al.*, 2004; Yemshanov *et al.*, 2005; Daigneault *et al.*, 2010). In North America, afforestation is considered a cost-effective and ecologically viable option to sequester atmospheric CO₂ due to the significant presence of marginal and abandoned agricultural lands (Parker et al., 2009; Gale et al., 2013). In fact, many studies have evaluated the economic feasibility of afforestation in North America, but assessments that attempt to account for carbon (C) sequestration through direct linkages to growth processes and their dependence on seasonal and inter-annual climate variations are

lacking. Past studies (eg. van Kooten et al., 1995; McKenney et al., 2004; Yemshanov et al., 2005; Yemshanov et al., 2007; Kula and Gunalay, 2012) tend to utilize generalized forest growth and yield curves, which do not account for climate variability and extreme weather events.

Excluding climate variability is problematic because seasonal and inter-annual climate variability, as well as long-term changes in forest productivity due to climate change, will play a pivotal role in the growth and productivity of forest ecosystems (EPA, 2013). For example, increases in atmospheric CO₂ concentration and temperature may cause trees to be more productive due to a higher rate of photosynthesis – as long as sufficient water and nutrients are available (Backlund *et al.*, 2008; Johnston *et al.*, 2009). Warming temperatures may also increase growing season length, and allow some tree species to move northward or to higher altitudes (Backlund *et al.*, 2008). Alternatively, climate change may result in lower forest productivity and higher mortality due to an intensification of disturbance events, such as forest fire, insect pests, and drought (Price et al. 2013). Understanding and quantifying productivity changes for particular species in both natural and managed situations is clearly a complex and highly uncertain scientific problem.

Global climate models represent an integration of various biophysical processes and attempt to fully account for climate variability (Hansen et al., 1983; Hansen et al., 1984). These models have the ability to simulate the response of the climate system to increasing

greenhouse gas concentrations and provide future climate projections under different greenhouse gas emission scenarios (Schmidt et al., 2006; IPCC 2013; Schmidt et al., 2014). Response variables related to carbon budgeting of terrestrial ecosystems include gross primary production (GPP), net primary production (NPP) and net ecosystem production (NEP). In forest ecosystems, approximately 50% of atmospheric carbon assimilated through photosynthesis (i.e. GPP) is considered to be allocated to live plant components, which is known as NPP (He et al., 2012; IPCC, 2000). This means that remaining 50% of GPP or assimilated carbon is lost through ecosystem respiratory processes, including live plant components or autotrophic respiration (R_a) and turnover of both aboveground and belowground dead plant components and soil organic matter, known as heterotrophic respiration (R_h) (IPCC, 2014). The term NPP – which represents the net production of biomass in the process of photosynthesis – often equates with plant growth as NPP provides estimates for a biomass or carbon assimilation rate (Pretzsch, 2009; He et al., 2012). Assimilated carbon can be used as a source of energy for trees to grow (Pretzsch, 2009). NEP represents the net accumulation of carbon by an ecosystem; which is the difference between NPP and R_h (IPCC, 2014). NEP can thus be used to estimate carbon sequestration in a given area over a given period.

Looming climate change impacts have given rise to a growing interest in carbon pricing. By putting a price on greenhouse gas emissions, individuals and organizations have a clear financial incentive to minimize the costs of consuming carbon embedded in energy. The two most popular methods of carbon pricing are a carbon tax and a cap-and-trade

system. A carbon tax is a tax-based scheme on greenhouse gas (GHG) emissions generated from burning fossil fuels. Essentially, it puts a monetary price on each ton of carbon emitted to the atmosphere (BC's Climate Action Plan, 2007; World Bank, 2014). A cap-and-trade system is a government-mandated approach in which a limit, or cap, is placed on the amount of carbon emitted by the industrial units, with the cap lowered over time to reach a set emission target (World Bank, 2014; Rydge, 2015). Both approaches, if well-designed and implemented, can encourage industries and consumers to reduce GHG emissions as they are faced with the full social costs of their actions. Ontario is currently implementing a cap-and-trade system which may have implications for the forest sector.

Several studies have examined the effect of carbon taxes and subsidies on optimal forest harvest rotation periods when both timber and carbon sequestration benefits are considered (Hoen, 1994; van Kooten et al., 1995; Hoen and Solberg 1997; Stainback and Alavalapati, 2002; Asante and Armstrong, 2012). In these models, landowners receive a subsidy for the amount of carbon sequestered in forest biomass and are taxed when sequestered carbon is released back into the atmosphere through harvest. In fact, studies show that carbon taxes and subsidies generally influence the optimal harvest rotation by postponing the harvest (Plantinga and Birdsey, 1994; Englin and Callaway, 1995; Enzinger and Jeffs, 2000). To our knowledge, no published studies have integrated plant productivity projections from GCMs into forest planning tools to estimate future forest yields and related economic values.

This study integrates forest productivity estimates simulated by the process-based ecosystem models used in GCMs with a spatial forest investment model to examine future projections of forest productivity and related economic values. The specific objectives of this study are to: (i) generate future merchantable timber yield estimates for black spruce that account for climate variability utilizing global climate model simulated NPP estimates; (ii) examine the economic potential of black spruce plantations, inclusive and exclusive of carbon sequestration benefits in Ontario, Canada; and (iii) conduct a sensitivity analysis to determine how uncertainty in the model input parameters affects the economic attractiveness of investing in black spruce plantations under climate change. Current and future forest productivity estimates from three different process-based global climate models were used. The investment attractiveness is judged by net present value (NPV) calculations via cost-benefit analysis (CBA) (Boardman et al., 2001). CBA is an assessment method that measures the value of projects in monetary terms. It is used to help decision making processes and clarify which potential policies or projects are the most efficient (Boardman et al., 2001). In our study, the use of NPV via CBA conveys whether black spruce plantation investments are financially attractive with or without carbon pricing.

CHAPTER 2: DATA AND METHODS

2.1 Overview

The analysis required the development and integration of data from several sources. An overview of the steps is shown in Figure 1, illustrating the integration of the

biogeophysical model, the specific black spruce forest growth and yield model, and the economic analysis to generate present value estimates. We used temporal and spatial distribution of GCM simulated NPP to modify gross merchantable timber volume trajectories obtained from the black spruce growth and yield model. Annual NPP estimates were extracted from three different GCMs – CanESM2 (Canadian), MIROC (Japanese), and MPI (European). The study focused on the province of Ontario in eastern Canada below 52° latitude (Figure 2), which marks the northern boundary of the province’s active forest management zone (OMNR, 2013). Although deep southern Ontario is not part of the active forest management zone, or part of black spruce’s natural range, we include this region to help illustrate variation in these types of calculations across this broad spatial domain. Net present values were generated with and without carbon sequestration values. Carbon flows were generated based on the growth of NEP as it represents how much carbon is being stored in an ecosystem (IPCC, 2013). A baseline scenario of plantation investment costs, wood and carbon prices, and a discount rate to reflect the time cost of money were used for the calculations. Sensitivity analyses were used to examine the impact of the various parameters on the model outputs. NPV calculations follow the basic Faustmann model (see Faustmann, 1968) for the wood production values and a modified Hartman model for the carbon value calculations (Hartman, 1976; van Kooten et al., 1995). Further details are provided below.

2.2 GCM-Simulated NPP

The GCMs employed here are considered ‘coupled’ in that they link an atmospheric general circulation model with ocean, sea ice, and land surface models through the exchange of energy, momentum, water and important gases such as CO₂. Model simulation output for GCM-CanESM2 was obtained from the Canadian Centre for Climate Modelling and Analysis (CCCma; Taylor et al., 2009; <http://www.cccma.ec.gc.ca/data/cgcm4/CanESM2/index.shtml>). CanESM2 includes a process-based dynamic vegetation model, known as the Canada Terrestrial Ecosystem Model (CTEM), the fourth generation atmospheric general circulation model (CanCM4), the physical ocean component (OGCM4), and the Canadian Model of Ocean Carbon (CMOC; Christian et al., 2010) (Arora and Boer, 2010; Gillett et al., 2012). Model simulations were performed at rather coarse resolution, 2.8° X 2.8° (Gillett et al., 2012; Separovic et al., 2013; Arora and Boer, 2014). Model grids for the study area based on this resolution are shown in Figure 2a.

GCM-MIROC (Model for Interdisciplinary Research on Climate) has been developed by the University of Tokyo, NIES, and JAMSTEC (Nozawa et al., 2007; Watanabe et al., 2011) and consists of multiple components: atmospheric general circulation model (MIROC-AGCM), an aerosol component (SPRINTARS v5), an ocean GCM with sea-ice components (COCO v3.4), and a land surface model (MATSIRO) (K-1 model developers, 2004; Watanabe et al., 2011). MIROC shares the same spatial resolution as CanESM2.

GCM-MPI (Max-Planck-Institute) consists of multiple components: atmospheric general circulation model (ECHAM6; Stevens et al., 2013), an ocean model (MPIOM; Jungclaus et al., 2013), a land model describing physical and biogeochemical aspects of soil and vegetation (JSBACH; Giorgetta et al., 2013; Reick et al., 2013), and marine geochemistry model (HAMOCC5; Ilyina et al., 2013). This model includes the carbon cycle which allows studying the impacts of climate change on the carbon cycle (Giorgetta et al., 2013). The spatial resolution of MPI model simulations was $2.5^{\circ} \times 2.5^{\circ}$. Figure 2b shows the grid created for the study site based on this resolution.

These GCM simulations were performed from 2006 to 2100 for different future climate scenarios under CMIP5 initiative and IPCC AR5 report (Taylor et al., 2009; IPCC, 2014). These future climate trajectories are based on four different future projections of greenhouse gas concentrations, known as Representative Concentration Pathways i.e. RCP2.6, RCP 4.5, RCP 6.0, and RCP 8.5 (IPCC, 2014). Each RCP defines a specific emissions pathway and subsequent radiative forcing, which represents a cumulative measure of human emissions of GHGs in the Earth-atmosphere system – expressed in Watts per square meter (Wayne, 2013). From lowest to highest, RCP scenarios represent mitigation (RCP2.6), two moderates (RCP 4.5 and 6.0), and a more extreme scenario (RCP8.5). CO₂ concentrations for RCP scenarios are estimated to reach 421, 538, 670, and 936 ppm (parts per million) by 2100, respectively (Jones et al., 2013).

In this study, we used NPP projections under the RCP 8.5 trajectory (extreme scenario) because GHG emissions are currently tracking those associated with this scenario (Sanford et al., 2014). Also, the extreme scenario provides the best-case, or potentially the worst-case, scenario to estimate the potential economic investment values.

The simulated NPP from these three different GCMs was used to estimate future merchantable timber yields for black spruce forest ecosystems as described in detail in the following section.

2.3 Growth and Yield estimates and NPP adjustments

Growth and yield expectations under a rapidly changing future climate are an active area of research. Researchers have investigated different methods, ranging from statistical analyses between climate variables and yields (e.g., Ung et al., 2009) to biological process-based approaches (e.g., Girardin et al., 2008; Coulombe et al., 2010). Some scientists argue that a warming climate could result in a potential decrease in forest productivity (Girardin et al., 2008), while other studies show otherwise (Shugart et al., 2003; EPA, 2013).

Conifers are typically used for timber production due to their somewhat lower establishment and management costs and high potential harvest value (Yemshanov et al., 2005). Depending on the species, site conditions and management practices northern conifers typically have longer rotation periods ranging from 40 to 80 years (or more in

some cases). For our study, growth functions for black spruce were obtained through Ung et al.'s equation. They were developed to assess changes in standing volume across Canada's forests (Ung et al., 2009).

$$\ln(V) = \beta_0 + \beta_1 D + \beta_2 P + \frac{\beta_3 + \beta_4 T + \beta_5 P}{t} \quad [1]$$

$$V = \exp[\ln(V)] * C_d \quad [2]$$

where V represents gross total volume of live merchantable trees ($\text{m}^3 \text{ ha}^{-1}$), t represents plot age (years), D represents mean annual temperature ($^{\circ}\text{C}$), P represents annual mean precipitation (mm), C_d represents the Duan correction factor (Duan, 1983) and β represents parameters for different species. This equation takes climate variability, such as temperature and precipitation, into account and therefore should provide more realistic spatial variation in volume estimates. Historical annual mean temperature and annual precipitation estimates (1961-1990) were obtained based on the center coordinates of each grid cell from Natural Resources Canada (McKenney et al., 2011).

Though Ung et al. (2009) incorporate temperature and precipitation into their yield models, the authors warn that their equations are not intended for use under climate change. The reason for this is that climate change is expected to produce novel climatic conditions that could push the models outside the range of conditions for which they were originally developed. A good example of this is the equation for black spruce, which predicts increasingly high yields under climate change, regardless of how high the mean annual temperature becomes. Therefore, Ung et al. (2009) yield model for black spruce

may not adequately account for temperature feedbacks that cause growth to decline after a certain temperature is reached.

Conversely, NPP simulated by the process-based ecosystem models used in the GCMs account for future climate changes; however, these estimates are for general plant or forest growth (C3 species) and do not fully represent black spruce as forest species. Therefore, we developed a hybrid approach that incorporated both the GCM simulated NPP and Ung et al. (2009) growth estimates for black spruce forests. First we calculated an NPP modifier as a ratio of future to current NPP as shown below:

$$R_{NPP} = \frac{NPP_{predicted}}{NPP_{baseline}} \quad [3]$$

The NPP ratio (R_{NPP}) is calculated annually for each grid cell using the GCM-simulated past NPP estimates from CMIP5 and IPCC AR5 data sets from 1970 to 2000 ($NPP_{baseline}$) and the predicted future NPP for each year over the 2011 to 2100 period ($NPP_{predicted}$). R_{NPP} ranges between 0 to ∞ where a value between 0 and 1 indicates a decrease in NPP and any value higher than 1 indicates an increase in NPP. R_{NPP} is multiplied by the change in volume over each year and then added onto the total volume accumulated in previous years:

$$V(t) = R_{NPP} * (V(t) - V_{(t-1)}) + V_{Tot} \quad [4]$$

Note that the black spruce yield volumes in equation 4 are calculated using the Ung et al. (2009) equation with historical mean annual temperature and annual precipitation estimates set to current values (i.e., 1961-1990) obtained for each grid cell from Natural Resources Canada (McKenney et al., 2011). Annual yields were estimated for all grid

cells across the study area, based on a plantation initiation date of 2016. In order to illustrate the yield volume spatially, we employed the grids of 1961-1990 mean annual temperature and annual precipitation described above to calculate black spruce volume in the absence of climate change using the Ung et al. (2009) equation and then modified these estimates using the NPP ratio modifier.

2.4 Harvest Models and Economic Calculations

As noted, NPV was used as a metric to quantify the value of growth and yield investments by aggregating geophysical and economic flows from a standing forest that could arise over a forest's growth period. NPV was calculated using two different harvest models – the Faustmann model which considers only revenues from wood production (Faustmann, 1968; Samuelson, 1976), and a modified Hartman model which includes both carbon sequestration revenues and wood production (see Hartman, 1976). Because the exact price of carbon is still unknown or yet to be defined in Canada, we used a range of values from Canadian \$5 to \$20 $\text{ton}^{-1} \text{CO}_2$. In 2006, carbon prices were \$3.36 (US \$3) $\text{ton}^{-1} \text{CO}_2$ at the Chicago Climate Exchange (Yemshanov et al., 2007). In 2016, carbon prices are US \$12.50 $\text{ton}^{-1} \text{CO}_2$ at the California Carbon Dashboard (California Carbon Dashboard, 2016). The \$5 $\text{ton}^{-1} \text{CO}_2$ is therefore perhaps a reasonable starting point for the carbon sequestration scenarios. Finally, for descriptive purposes, the NPVs were then organized by dividing Ontario into three regions – northwest, northeast, and southern Ontario. Figure 2a shows how grids of Ontario for CanESM2 and MIROC are divided where -87.4 decimal degrees longitude is used for a division between NW and NE

Ontario and 47.4 decimal degrees latitude is used for a division between northern and southern Ontario. Figure 2b shows the division of grids of Ontario for MPI where -86.4 decimal degrees longitude is used for a division between NW and NE Ontario and 48.4 decimal degrees latitude is used for a division between northern and southern Ontario.

2.4.1 Faustmann Model

The Faustmann model or formula was developed by German forester Martin Faustmann in 1849. The formula provides the theoretical basis for optimal harvest age decisions (Johansson & Lofgren, 1985; Cairns, 2012). It calculates the net present value of the timber using inputs such as the discount rate (time cost of money investments), standing timber values, establishment costs, and merchantable timber volumes. The model determines the optimal harvest age by identifying the period when NPV is maximized over an infinite series of rotations (Faustmann, 1968; Samuelson, 1976; Chang, 1998; Cairns, 2012). In our study, we assume that the forest is managed under 21st century climate and an infinite cycle of establishment, growth, and harvests. The NPV of standing timber is

$$NPV = \frac{[PV(t)-C]e^{-rt}}{1-e^{-rt}} - C \quad [5]$$

where NPV is the net present value (\$ ha⁻¹), P is the stumpage or standing timber value (\$ m⁻³), V(t) is the yield equation (m³ ha⁻¹), C is the establishment cost (\$ ha⁻¹), r is the discount rate or time value of money (%), and t is the age of forest. For a baseline scenario, the price of stumpage is set to \$20 m⁻³, stand establishment cost is set to \$500 ha⁻¹, and the discount rate is set to 4%. The first order condition for the optimal harvest

age can be found by differentiating equation [5] with respect to harvest age, t , which represents the relative rate of value growth. When the first order condition is set to zero and solved for t , it identifies the rotation age that maximizes NPV over a harvest cycle. This effectively identifies the highest point on the NPV curve where the slope is equal to zero. The first order condition is

$$\frac{V'(t)}{[V(t) - \frac{C}{P}]} = \frac{r}{1 - e^{-rt}} \quad [6]$$

The left hand side of equation [6] refers to the relative value growth rate (RVGR) and the optimal harvest age should be chosen when the RVGR is equal to the discount rate. If the landowner is interested in pursuing an economic approach to stand management he/she will maintain the stand if the return values are greater than the interest rate, and harvest the stand before the investment yield drops below the market rate. We used the simple model in Figure 3 to illustrate the comparative static analysis to observe how the variables (*i.e.* P , C , r and V) affect the optimal rotation period. If the RVGR curve shifts upward, the optimal harvest age is going to increase. If the RVGR curve shifts downward, the optimal harvest age is going to decrease. When P increases, it increases the denominator of the left hand side (LHS) lowering the overall RVGR. This causes the RVGR curve to shift downward making the optimal harvest age younger. Conversely, increasing C decreases the denominator of LHS making the overall RVGR higher and therefore the optimal harvest age increases. If discount rate increases, the horizontal line moves up causing the harvest age, the intersection point, to decrease.

For the models presented here, we assume that trees would not be harvested until V reaches at least $80 \text{ m}^3 \text{ ha}^{-1}$ because trees need to reach a certain level of volume in order to be considered as merchantable by forest industry (McKenney et al., 2013; Gauthier et al., 2015).

2.4.2 Incorporating Carbon Sequestration Value:

The Faustmann model does not consider other values that forests can offer, such as ecosystem, environmental and recreational services and C uptake benefits. The Hartman model (Hartman, 1976) allows the formulation of economic assessments of the optimal harvest age of a forest, when both timber value and flows of other important services are provided by forest stands. Depending on the values under consideration, the optimal age may be before or after the optimal harvest age for wood production. Indeed, in principal, it may be optimal not to harvest the stand. One of many services includes the value of carbon sequestration (van Kooten et al., 1995). The rate at which a forest sequesters C is proportional to the growth of the forest.

As noted previously, NEP represents the net accumulation of carbon by an ecosystem (IPCC, 2014). C benefits are a function of the changes in biomass and the amount of C per cubic meter (m^3) of biomass (van Kooten et al., 1995). A conversion factor of 0.3 is used to reduce the total carbon mass accumulated by the ecosystem to merchantable wood volume, roots, and soil conditions (Jessome, 1977; Asante and Armstrong, 2012).

Present values of the flow of C uptake benefits over the period of t are calculated as below:

$$PV_C = P_{cs} \int_0^t F'(t) \beta_c e^{-rt} dt - P_{cs} F(t) e^{-rt} \quad [7]$$

where PV_C is the present value of the C sequestration, P_{cs} is the carbon price (\$ ton⁻¹ CO₂), $F(t)$ is the C sequestration function, β_c is the conversion factor, 0.3, to reduce the total carbon mass to biomass volume which is consistent with an estimated carbon content of wood of approximately 200 kg m³ (Jessome, 1977), r is the discount rate (%), and t is the age of the forest. The term to the left of the minus sign of eq. [7] represents the NPV of carbon stored over the period of the standing trees, whereas the term to the right represents the payment that must be made when the stand is harvested as forest biomass is expected to be set to zero at the time of harvest (Asante and Armstrong, 2012). $F(t)$ is the mass of carbon in standing trees (biomass, ton ha⁻¹) as a function of stand age, given by:

$$F(t) = v_1(1 - e^{-v_2 t})^{v_3} \quad [8]$$

in which v_1 , v_2 , and v_3 are parameters, which are set at 189.6, 0.0268, and 2.56 respectively. This equation was fitted to simulated NEP data over the 1901 to 2100 periods.

Inserting eq. [7] to the Faustmann model (eq. [5]) gives the NPV of both timber production and the flow of C sequestration value:

$$NPV = \frac{[PV(t) - C]e^{-rt} + P_{cs} \int_0^t F'(t) \beta_c e^{-rt} dt - P_{cs} F(t) e^{-rt}}{1 - e^{-rt}} \quad [9]$$

As noted we used a fixed carbon price of \$5 ton⁻¹ CO₂ due to the fact that carbon markets are not well established yet. In sensitivity analyses, we increased the carbon price to \$10 and \$20 ton⁻¹ CO₂. The calculation gives the optimal harvest age that maximizes NPV of both timber and non-timber benefits, in this case carbon. The first order conditions for a optimization is

$$\frac{V'(t)}{\left[V(t) - \frac{C}{P}\right] - P_{CS}F(t)} = \frac{r}{1 - e^{-rt}} \quad [10]$$

Given that $F(t)$ increases with time and that carbon price is positive, LHS of eq. [10] is always larger than LHS of eq. [6]. This indicates that the relative growth rate curve for a modified Hartman model is always above the relative growth rate curve for a Faustmann model. For any discount rate, therefore, the optimal harvest age will always be older when carbon benefits are included as compared to the timber-only scenario.

2.5 Sensitivity analysis

Sensitivity analyses are a useful tool to examine possible outcomes where uncertainty is inherent in the problem formulation. In this case, we have used it to explore the response of NPV to parameter uncertainty. For each model parameter, simulations were repeated with the parameter adjusted within a reasonable range from its original values. This shows the relative sensitivity of NPVs to the decrease or increase of the particular parameter value. Table 1 summarizes the assumptions for the growth and yield scenarios that were applied to all economic models and sensitivity analyses

CHAPTER 3: RESULTS AND DISCUSSION

3.1 NPP and Growth Projection

Annual NPP projections of the three different GCMs from 2006 to 2100 are shown in Figure 4. Both CanESM2 and MPI show a gradual increase in NPP over time, but the rate at which NPP increases is higher for MPI. MIROC, however, predicts a decrease in NPP in the second half of the century with greater inter-annual variability. According to Liu et al. (2002), average NPP in eastern Canada is approximately $259 \text{ g C m}^{-2} \text{ year}^{-1}$; however, GCM simulated NPP values are rather small only reaching a maximum of $\sim 170 \text{ g C m}^{-2} \text{ year}^{-1}$. This issue arises because models use single representations of land cover to describe large grid cells which could result in overestimation/underestimation. Although the issue could be resolved with a higher resolution, we were limited by the coarse resolution provided in the GCM outputs (Skidmore, 2002). Figure 5 shows the spatial distribution of NPP estimates in the study area for every 10th year over the 2020 to 2100 period. The NPP distributions are shown for each decade in order to capture temporal patterns as well. In all three models, there is a clear Northwest-Southeast gradient, where NPP is higher in the southeastern region than the northern region. Highest NPP estimates are often found in the region east of Lake Huron. This is likely due to the influence of higher temperature and greater precipitation in those regions (Rossi et al., 2011; Rossi et al., 2014; Girardin et al., 2016). Experimental studies have also reported that carbon assimilation by black spruce trees may increase from climate warming due to a positive correlation between tree radial increments and temperature (Bronson et al., 2009; Gennaretti et al., 2014; Ueyama et al., 2015). Although it is possible that these responses may be inhibited by other warming induced processes affecting plant growth such as

water limitations on photosynthesis due to drought (Way and Sage, 2008; Zhang et al., 2008).

Figure 6 shows the spatial distributions of the adjusted gross merchantable volumes of black spruce in the study area based on GCM-simulated NPP ratios, and meteorological variables. The years prior to 2040 are not shown because black spruce yields in the study area have not yet reached the $80 \text{ m}^3 \text{ ha}^{-1}$ harvest minimum described above. Overall, there is a clear North-South gradient in volume growth, with gross merchantable wood volume increasing as you move southward. The projected average yield volumes in 2100 for CanESM2, MIROC, and MPI in southern Ontario are 270, 277, and $253 \text{ m}^3 \text{ ha}^{-1}$, respectively. The projected average yield volumes in 2100 for CanESM2, MIROC, and MPI in northern Ontario are 170, 170, and $156 \text{ m}^3 \text{ ha}^{-1}$, respectively. This north-south productivity gradient is driven by a combination of higher NPP, mean annual temperature, and annual precipitation in the southern region (Fang et al., 2001; Del Grosso et al., 2008; Zhu and Southworth, 2013). In order to validate the yield estimates from the Ung et al. (2009) equation, we used Plonski's (1956) normal yield tables which provide detailed information on various characteristics of black spruce growth and yield in Ontario as a function of stand age – including diameter at breast height (DBH), height, gross merchantable volume, and more (Plonski, 1956; Payandeh, 1991). According to these tables, gross merchantable volumes for 100-year-old black spruce stands in Ontario are expected to range from $\sim 120 \text{ m}^3 \text{ ha}^{-1}$ to $\sim 230 \text{ m}^3 \text{ ha}^{-1}$, depending on site productivity. Other yield studies also suggest that volumes of $\sim 200 \text{ m}^3 \text{ ha}^{-1}$ are possible in 80- to 100-

year-old stands in southern Canada and the regions surrounding Great Lakes under normal managed good site conditions (Fowells, 1965). Given the relatively extreme climate scenario (RCP 8.5) in our study, the projected average yield volumes for three GCMs appear reasonable. In comparison to the generalized growth and yield curves, results generated from the hybrid approach incorporating GCM-simulated NPP and Ung et al.'s (2009) equations capture inter-annual variability, creating noise in model outputs. Depending on the spatial- and temporal-scale, results may vary from ~ 20 to $\sim 40 \text{ m}^3 \text{ ha}^{-1}$ each year resulting in overestimation/underestimation of gross merchantable volumes.

The simulated NPP from three different GCMs is used to project future NPP changes for a coming century and to estimate its subsequent effect on forest productivity and ultimately merchantable timber yields. These model predictions, however, have limitations as there is a lack of understanding of the atmospheric processes controlling carbon allocation (Waring and Running, 2007). The effect of CO_2 and water availability on GPP is interrelated. CO_2 -enrichment studies have suggested that plant productivity increases by 20% to 50% when CO_2 is doubled given adequate nutrients and water (Kimball, 1975; Gates, 1985; Xiao et al., 1996). In general, increasing CO_2 and water availability increases GPP, which in turn increases NPP and affects plant growth.

Temperature also plays an important role when it comes to GPP. When air temperature is within a tolerable range – between the optimum temperature and a maximum vegetation-specific temperature constraint – it has a positive impact on plant productivity. However, when air temperature increases beyond this maximum constraint, it quickly results in

reduced plant productivity (McGuire et al., 1996; Xiao et al., 1996). Moreover, temperature affects R_a since R_a generally increases logarithmically with temperature (McGuire et al., 1992; Xiao et al., 1996).

3.2 Economic benefits

Figure 7 shows the spatial representation of net present values of black spruce exclusive of carbon values in the study region using the Faustmann model. The figure clearly illustrates the effect of spatial variation in meteorological variables on land values. The optimal harvest ages for CanESM2, MIROC, and MPI are 39, 38, and 38 years, respectively for the baseline scenario. These rotation ages are well below typical rotation ages for this species (e.g., maximum sustained yields – MSY – as discussed in Yang et al., 2015), but the MSY rotation does not include any economic value considerations. At these optimal economic harvest ages, the average net present values for CanESM2 in northwest, northeast, and southern regions of the study are $-\$136$, $-\$265$, and $-\$51 \text{ ha}^{-1}$, respectively. Similarly, NPVs for these regions using MIROC are $-\$137$, $-\$269$, and $-\$39 \text{ ha}^{-1}$; and using MPI are $-\$226$, $-\$263$, and $-\$90 \text{ ha}^{-1}$ respectively. In general, as might be expected, NPVs are higher in southern Ontario in all three GCMs but all these models suggest silvicultural investments in black spruce are not attractive given the baseline economic assumptions used here. Interestingly, despite the decline in projected NPP in the second half of the century by the MIROC model, both optimal harvest age and NPVs do not vary much from the other two GCMs. This is rather unexpected as it was initially thought that the NPP modifier would play a critical role in determining the optimal

rotation age and economic attractiveness of the simulated plantations. However, in hindsight, it is clear that the discount rate greatly reduces the impact of the NPP modifiers, which are largest toward the end of the century. Differences in spatial resolution also had small effect on NPV results. In previous section, it was mentioned that merchantable volume differences between CanESM2 and MIROC (~2.8°), and MPI (~2.5°) are ~20 m³ ha⁻¹. Despite having slightly higher resolution – which has the potential to improve the precision and accuracy of the results – the NPV maps for MPI do not differ much from those of CanESM2 and MIROC. Overall, the wood value-only results appear insufficient to attract forest plantation investors.

Figure 8 shows the map of NPVs of black spruce inclusive of carbon benefits based on the modified Hartman model. The optimal harvest ages for CanESM2, MIROC, and MPI are 42, 44, and 42 years, respectively. Overall, the optimal harvest ages become longer when carbon benefits are included in the model. In comparison, Yemshanov et al. (2005) reported an optimal rotation age of 49 years for coniferous forests in eastern Canada inclusive of carbon benefits. Yemshanov et al. (2005) used the outputs from a carbon tracking model to calculate carbon sequestration benefits. This allowed estimation of net annual carbon sequestration from numerous carbon pools, whereas our study depends solely on simulated NEP for quantifying carbon sequestration. Despite these different approaches to quantifying carbon sequestration, our final NPV values appear reasonable.

The summary of NPVs of timber inclusive and exclusive of carbon values by regions is shown in Table 2.

Average NPVs at their optimal harvest age for CanESM2 in northwest Ontario, northeast Ontario, and southern Ontario are \$430, \$305, and \$522 ha⁻¹, respectively. NPVs for these regions using MIROC are \$424, \$304, and \$529 ha⁻¹, respectively, and using MPI are \$341, \$306, and \$485 ha⁻¹, respectively. A price of \$5 ton⁻¹ CO₂ does appear to be the minimum threshold to begin to make black spruce silvicultural investments attractive (see also Yemshanov et al., 2005). This suggests that the overall investment results heavily rely on the carbon price assumptions. It is important to note that; depending on the models that different studies use, NPV outputs should vary between timber-only and timber-and-carbon scenarios. These maps should only be used as general indicators of relative potential value due to the coarse scale of the spatial inputs used in the study.

A limitation of the current work is that we assume that the carbon sequestration value never decreases with age. A number of studies have indicated that water limitations and heat stress may limit the ability of black spruce to grow and sequester carbon, but there is no consensus on the impacts of future climate warming on the productivity of black spruce and forests in general (Girardin et al., 2008; Zhang et al., 2008; Johnstone et al., 2010; Beck et al., 2011). Girardin et al. (2016) looked at the impacts of climate warming, drying, and increasing CO₂ on the productivity of black spruce forests between the period of 1971 and 2100. They looked at the future responses of a tree growth index (TGI) and

model-simulated NPP to climatic fluctuations and reported black spruce inter-annual variability in productivity is highly driven by soil water availability in cold northern regions and by autotrophic respiration in warm southern regions. The study summarized that soil water availability and respiration are the limiting factors on future NPP over the next century. Therefore, it is plausible to assume that pending climate change could potentially result in decrease in carbon uptake value and affect the overall plantation investments.

3.3 Sensitivity Analyses

Sensitivity analyses were performed for both wood-only and wood + carbon scenarios to determine the effect of economic uncertainty on model results. Table 3 summarizes the sensitivity analyses of the wood-only scenario for a range of r , C , and P values. When r is increased from 4% to 8%, all three models – CanEMS2, MIROC, and MPI – indicate shorter rotation periods: from 39 years to 33 years, from 38 years to 33 years, and from 38 years and 32 years respectively. Furthermore, because the time value of money is increased, NPVs significantly drop at their new adjusted optimal harvest ages. The highest drop in NPVs is observed in the southern region of the study area, whereas the least is seen in northeastern region for all three GCMs. Conversely, when r is decreased from 4% to 2%, all models suggest that longer rotation periods are appropriate: from 39 years to 46 years for CanESM2, 38 years to 45 years for MIROC, and 38 years to 46 years for MPI. Here, there is a drastic increase in NPV in southern Ontario, with a smaller increase in the northeastern region. The results imply that the more southern regions of

the study area are the most sensitive to changes in r when it comes to future black spruce silviculture investment. C was adjusted from \$500 to \$200 and \$1000. When C is reduced to \$200, the rotation periods become shorter: from 39 years to 35 years for CanESM2, from 38 years to 36 years for MIROC, and from 38 years to 36 years for MPI.

Furthermore, NPVs for the three GCMs show increases that are comparable to the reduction in C , which is ~\$300. Conversely, when C is increased to \$1000, the rotation periods become longer by 7 to 8 years depending on the models. The increased establishment cost makes the overall investment questionable for all three GCMs. This has been shown in other studies as well, where the economic attractiveness of plantations increases in areas where opportunity costs (e.g., land values) are low (Yemshanov et al., 2007). Lastly, when P is adjusted from \$20 to \$50, the result is a shorter rotation period by 2 to 5 years depending on the GCM. Increasing P turns NPV from negative to positive, making the investment more attractive. Although the increases in NPVs vary by regions, the highest present values remain primarily in southern parts of study area and lowest in northeastern Ontario.

Table 4 illustrates the results of the sensitivity analyses of the wood + carbon scenario, where r , C , P and P_{cs} are adjusted to observe the effects of parameter uncertainty on the resulting NPVs. First we decreased r from 4% to 2% and observed longer rotation periods by 3 to 7 years depending on the GCM. NPV also increased drastically; in the southern region of the study site, it increased by \$1,000. When r is changed from 4% to 8%, we observed shorter rotation periods for all three GCMs and NPVs are reduced making the

overall investment debatable. When carbon sequestration benefits are included in the model, the RVGR curve in figure 3 is raised and therefore the curve is always going to be higher than the curve for the Faustmann model. This causes a delay where the intersection occurs resulting in longer rotation periods at any discount rate. When C is adjusted, similar trends occur: as C increases, the rotation periods become longer and NPVs go down by the differences in C . When P is adjusted from \$20 to \$50, the rotation periods become shorter by 4 to 9 years depending on the GCM. However, NPVs increase by almost 10 fold in southern Ontario, making the investment extremely attractive. The optimal harvest age increases with increasing carbon prices. This can be interpreted as a way to postpone the penalty associated with re-releasing the carbon to the atmosphere at harvest (Asante and Armstrong, 2012). In comparison to the Faustmann model results, NPVs increase considerably, indicating the significance of including C uptake benefits in this investment. We note that, with increasing P_{cs} , changes in NPV are not as large as perhaps initially thought. These potential P_{cs} , however, provide evidence for the cost-effectiveness of afforestation efforts, which could be compared to other possible carbon sequestration activities. The results from sensitivity analyses also suggest that the discount rate is the most sensitive factor in determining the optimal harvest age and value. As black spruce regeneration processes require long run investments, the time value of money is very important here (Stern, 2007; Nordhaus, 2008).

3.4 Study Significance and Future Directions

Our results are portrayed spatially, which is often overlooked in economic analyses. Non-spatial analyses often apply average values over large areas, thus ignoring significant geographic variation of key biological and financial factors. This can be problematic because climate change affects ecosystems at multiple spatial scales – from local to global. Our use of GCM-derived NPP values and climate-driven yield equations allowed us to present results spatially – albeit at a relatively low resolution – and thus we were able to distinguish regions where black spruce regeneration investment should be most attractive.

Based on these findings, investments in black spruce plantations for timber production appear rather unattractive without the financial benefits of carbon sequestration. This indicates that implementing effective carbon pricing will be important for driving future interest in afforestation efforts. With growing interest and support for carbon pricing, governments, businesses and investors increasingly recognize the importance of well-designed carbon taxes and trading schemes that can reduce GHG emissions without negative economic impacts. In fact, around 40 countries and over 20 cities, states, and regions have implemented or laid the groundwork for a carbon pricing scheme (Rydge, 2015). The current work contributes to the ongoing effort to identify effective carbon sequestration prices and projects.

Another significant aspect of this study is that it incorporates inter-annual future climate variability into the growth and yield model, thus generating noisy, but more realistic,

forest growth and yield estimates. Past studies (eg. van Kooten et al., 1995; McKenney et al., 2004; Yemshanov et al., 2005) have utilized generalized forest growth and yield curves where seasonal and inter-annual climate variability are ignored. Interestingly, our findings suggest that the range of black spruce growth and yield estimates for the end of the current century using annual future climate inputs do not vary much from those obtained using standard curves (Payandeh, 1996; Payandeh and Wang, 1996).

Further research is required to quantify some of the risk factors associated with investments in forest plantations. In our study, risk factors such as wildfire, disease outbreaks, or drought were not included. However, inclusion of such factors would help to improve future estimates of the economic values associated with forest plantations. Martell (1979) indicated that when probabilistic fire occurrence is incorporated into a stochastic forest stand rotation model, it leads to shorter rotation intervals. Inclusion of forest fire risk is useful because fire is a major disturbance in the Canadian boreal forest that could impact large-scale patterns in biodiversity, carbon, vegetation, and forest management strategies (Daigneault et al., 2010; Boulanger et al., 2013). Daigneault et al. (2010) also observed that a probability of fire decreases rotation ages but when carbon prices are increased, rotation periods become longer despite a high probability of a fire.

Finally, GCM developers may incorporate nitrogen processes into their models to better assess the impacts of terrestrial productivity to climate variability and to focus on the feedbacks on forest ecosystem carbon sequestrations. Huang et al. (2011) indicated that

the simulation of nitrogen controls on carbon sequestration in conifer forests have shown a clear improvement in model outputs, which could help to reduce the uncertainty associated with future forest growth.

CHAPTER 4: SUMMARY AND CONCLUSIONS

Climate change will most likely have major impact on Canada's forest ecosystems. Given the important role of forests as a carbon sink in the global carbon cycle and the capacity to maximize the amount of carbon sequestered, afforestation is an important climate change mitigation strategy. Furthermore, there is a growing interest in carbon pricing, which can make efforts such as afforestation and reforestation attractive. This study explores the economic attractiveness of NPP-driven growth and yield investments for black spruce regeneration investments in Ontario, Canada under the assumption of a market for sequestered carbon in forest settings.

Future projections of NPP were obtained from three GCMs – CanESM2, MIROC, and MPI from 2006 to 2100 for extreme IPCC emission scenario (RCP 8.5). The study integrates process-based model simulated NPP, growth and yield model simulations, and economic analyses to investigate the overall investment values of black spruce – both inclusive and exclusive of carbon sequestration benefits. Future NPP trajectories indicate that both CanESM2 and MPI show a continuous increase in NPP, whereas MIROC shows a decline in NPP in the second half of the century. In all three models, however, there is a clear spatial North-South gradient across Ontario, with higher NPP in the southern than

the northern region. Despite the differences in temporal NPP trends and spatial resolution between GCMs, there are no notable differences in results, as it appears that final NPV estimates are not strongly impacted by these differences. Yield volumes by the end of the century under RCP 8.5 for the three GCMs are projected to be around $270 \text{ m}^3 \text{ ha}^{-1}$, which is somewhat greater than the average yield volume under normal managed conditions ($\sim 200 \text{ m}^3 \text{ ha}^{-1}$). Again, there is a clear North-South gradient in volume growth, with gross merchantable volume increasing as you move toward south.

The Faustmann model was used to calculate the optimal harvest age and the net present value of the timber. The results show that the rotation periods for CanESM2, MIROC, and MPI are 39 years, 38 years, and 38 years, respectively. Under the wood value-only scenario, and given the baseline assumptions used here, the overall investment would generally be unattractive due to negative NPVs across Ontario for all three GCMs. Even in the southern region of the study site, where the forest productivity is the highest, average net present values were negative; $-\$51$, $-\$39$, and $-\$90 \text{ ha}^{-1}$ for CanESM2, MIROC, and MPI, respectively.

When carbon benefits were introduced via a modified Harman model, the overall investment became financially attractive across the study region. The optimal harvest ages based on a modified Hartman model were 42 years, 44 years, and 42 years for CanESM2, MIROC, and MPI, respectively. Overall, as compared to the timber only model, the timber plus carbon model resulted in older optimal harvest ages for all three

GCMs. This can be thought of as a way to delay the penalty that must be made when harvest occurs as carbon is released back into the atmosphere. In southern Ontario, NPVs inclusive of carbon benefits are \$522, \$529, and \$485 ha⁻¹ for CanESM2, MIROC, and MPI, respectively. Furthermore, when carbon benefits were added, the optimal harvest rotation became longer at all discount rates; this was also noticeable in sensitivity analyses where rotations became longer as carbon prices increased. Overall, a minimum carbon price of \$5 ton⁻¹ CO₂ was required to make black spruce regeneration investments plausible. Through sensitivity analyses, we also found that discount rate plays an important role in the determination of optimal harvest age and value. Given that this study requires long run investments, the time value of money is extremely significant. In this study, we have not included risk factors that could affect growth and yield, such as drought and fire. Inclusion of these risk factors in future studies will demonstrate more realistic potential climate change impacts on forest plantation economics.

REFERENCES

- Arora, V., & Boer, G. (2010). Uncertainties in the 20th century carbon budget associated with land use change. *Global Change Biology*, 16(12), 3327-3348.
- Arora, V. K., & Boer, G. J. (2014). Terrestrial ecosystems response to future changes in climate and atmospheric co2 concentration. *Biogeosciences*, 11(15), 4157–4171.
<http://doi.org/10.5194/bg-11-4157-2014>
- Asante, P., & Armstrong, G. (2012). Optimal forest harvest age considering carbon sequestration in multiple carbon pools: A comparative statics analysis. *Journal of Forest Economics*, 18, 145–156.
- Backlund, P., Janetos, A., Schimel, D., Hatfield, J., Boote, K., Fay, P., Shaw, R. (2008). Introduction. In: *The effects of climate change on agriculture, land resources, water resources, and biodiversity*. A Report by the U.S. Climate Change Science Program and the Subcommittee on Global Change Research. Washington, DC., USA, 362 pp.
- Beck, P., Juday, G., & C, A. (2011). Changes in forest productivity across Alaska consistent with biome shift. *Ecology Letters*, 14, 373–379.
- Beer, C., Reichstein, M., Tomelleri, E., Ciais, P., Jung, M., Carvalhais, N., Papale, D. (2010). Terrestrial Gross Carbon Dioxide Uptake: Global Distribution and Covariation with Climate. *Science*, 329(5993), 834–838.
<http://doi.org/10.1126/science.1184984>
- Bigras, F. J., & Bertrand, A. (2006). Responses of *Picea mariana* to elevated CO₂ concentration during growth, cold hardening and dehardening: phenology, cold tolerance, photosynthesis and growth. *Tree Physiology*, 26, 875–888.
<http://doi.org/10.1093/treephys/26.7.875>
- Boardman, A., Greenberg, D., Vining, A., & Weimer, D. (2001). *Cost-Benefit Analysis: Concepts and Practice*. Prentice Hall. Upper Saddle River, NJ. 1-24.
- Boulanger, Y., Gauthier, S., Gray, D., Le Goff, H., Lefort, P., & Morissette, J. (2013). Fire regime zonation under current and future climate over eastern Canada. *Ecological Applications*, 23(4), 904–923.
- Cairns, R. D. (2012). *Faustmann's Formulae for Forest Capital*. McGill University. 1-23.
- Chang, S. (1998). A generalized Faustmann model for the determination of optimal harvest age. *Canadian Journal of Forest Research*, 28(5), 652–659.

- Climate Action Plan: British Columbia Ministry of Environment. (2007). Climate Action Plan. *Climate Action Plan*, 132. <http://doi.org/10.1038/news.2011.604>
- Coulombe, S., Bernier, P., & Raulier, F. (2010). Uncertainty in detecting climate change impact on the projected yield of black spruce (*Picea mariana*). *Forest Ecology and Management*, 259(4), 730–738.
- Daigneault, A. J., Miranda, M. J., & Sohngen, B. (2010). Optimal Forest Management with Carbon Sequestration Credits and Endogenous Fire Risk. *Land Economics*, 86(1), 155–172.
- Del Grosso, S., Parton, W., Stohlgren, T., Zheng, D., Bachelet, D., Prince, S., ... Olson, R. (2008). Global Potential Net Primary Production Predicted From Vegetation Class, Precipitation, and Temperature. *Ecology*, 89(8), 2117–2126. <http://doi.org/10.1890/07-0850.1>
- Duan, N. (1983). Smearing estimate: a nonparametric retransformation method. *Journal of the American Statistical Association*, 78, 605–610.
- Englin, J., & Callaway, J. (1995). Environmental impacts of sequestering carbon through forestation. *Climate Change*, 31(1), 37–78.
- Enzinger, S., & Jeffs, C. (2000). Economics of forests as carbon sinks: an Australian perspective. *Journal of Forest Economics*, 6, 227–249.
- EPA. (2013). Climate impacts on forests. Retrieved from <http://www.epa.gov/climatechange/impacts-adaptation/forests.html>
- Fang, J., Piao, S., Tang, Z., Peng, C., & Ji, W. (2001). Interannual variability in net primary production and precipitation. *Science (New York, N.Y.)*, 293, 1723. <http://doi.org/10.1126/science.293.5536.1723a>
- FAO. (2005). Global Forest Resources Assessment 2005. In *Food and Agriculture Organization*. Rome.
- FAO. (2010). Global Forest Resources Assessment 2010. In *Food and Agriculture Organization*.
- Faustmann, M. (1968). Calculation of the Value which Forest Land and Immature Stands Possess for Forestry. *Allgemeine Forst - Und Jagdzeitung*. 27-55.
- Fowells, H. (1965). *Silvics of Forest Trees of the United States*. U. S. Department of Agriculture, Agriculture Handbook no. 271. Washington, D.C.

- Gale, N., Trant, J., Schiks, T., L'Ecuyer, J., Jackson, C., Thevasathan, N., & Gordon, A. (2013). An economic analysis of afforestation as a carbon sequestration strategy in southwestern Ontario. *Studies by Undergraduate Researchers at Guelph*, 6(2), 55-65.
- Gates, D. (1985). Global biospheric response to increasing atmospheric carbon dioxide concentration. In: *Direct Effect of Increasing Carbon Dioxide on Vegetation*, B.R. Strain and J.D. Cure (eds.), 171–184.
- Gauthier, S., Bernier, P., Boulanger, Y., Guo, J., Guindon, L., Beaudoin, A., & Boucher, D. (2015). Vulnerability of timber supply to projected changes in fire regime in Canada's managed forests. *Canadian Journal of Forest Research*, 45(11), 1439-1447.
- Gennaretti, F., Arseneault, D., Nicault, A., Perreault, L., & Begin, Y. (2014). Volcano-induced regime shifts in millennial tree-ring chronologies from northeastern North America. *Proceedings of the National Academy of Sciences of the United States of America*, 111, 10077–10082.
- Gillett, N., Arora, V., Flato, G., Scinocca, J., & Von Salzen, K. (2012). Improved constraints on 21st-century warming derived using 160 years of temperature observations. *Geophysical Research Letters*, 39, 1-5.
- Giorgetta, M. A., Jungclaus, J. H., Reick, C. H., Legutke, S., Bader, J., Böttinger, M., ... Stevens, B. (2013). Climate and carbon cycle changes from 1850 to 2100 in MPI-ESM simulations for the coupled model intercomparison project phase 5. *Journal of Advances in Modeling Earth Systems*, 5(3), 572–597.
<http://doi.org/10.1002/jame.20038>
- Girardin, M. P., Hogg, E. H., Bernier, P. Y., Kurz, W. A., Guo, X. J., & Cyr, G. (2016). Negative impacts of high temperatures on growth of black spruce forests intensify with the anticipated climate warming. *Global Change Biology*, 627–643.
<http://doi.org/10.1111/gcb.13072>
- Girardin, M. P., Raulier, F., Bernier, P. Y., & Tardif, J. C. (2008). Response of tree growth to a changing climate in boreal central Canada: a comparison of empirical, process-based, and hybrid modeling approach. *Ecological Modeling*, 213(2), 209–228.
- Haavisto, V., & Jeglum, J. (1995). Black spruce in Ontario: an overview. *Natural Resources Canada, Canadian Forest Service-Ontario, Great Lakes Forestry Centre*. 1-4.

- Hansen, J., Lacis, a., Rind, D., Russell, G., Stone, P., Fung, I., ... Lerner, J. (1984). Climate sensitivity: Analysis of feedback mechanisms. *Climate Processes and Climate Sensitivity (AGU Geophysical Monograph Series 29)*, 5(29), 130–163.
- Hansen, J., Russell, G., Rind, D., Stone, P., Lacis, a., Lebedeff, S., ... Travis, L. (1983). Efficient Three-Dimensional Global Models for Climate Studies: Models I and II. *Monthly Weather Review*. 111(4), 609-662.
- Hartman, R. (1976). The harvesting decision when a standing forest has value. *Economic Enquiry*, 14(1), 52–58.
- He, L., Chen, J. M., Pan, Y., Birdsey, R., & Kattge, J. (2012). Relationships between net primary productivity and forest stand age in U.S. forests. *Global Biogeochemical Cycles*, 26(3), 1–19. <http://doi.org/10.1029/2010GB003942>
- Hoehn, H. (1993). The Faustmann rotation in the presence of a positive CO₂ price. *Journal of Forest Economics*, 35, 278–287.
- Hoehn, H., & Solberg, B. (1997). CO₂-taxing, timber rotations, and market implications. *Economics of Carbon Sequestration in Forestry*. 27, 151-162.
- Huang, S., Arain, M. A., Arora, V. K., Yuan, F., Brodeur, J., & Peichl, M. (2011). Analysis of nitrogen controls on carbon and water exchanges in a conifer forest using the CLASS-CTEMN+ model. *Ecological Modelling*, 222(20-22), 3743–3760. <http://doi.org/10.1016/j.ecolmodel.2011.09.008>
- Ilyina, T., Six, K., Segschneider, J., Maier-Reimer, E., Li, H., & Nunez-Riboni, I. (2013). Global ocean biogeochemistry model HAMOCC: Model architecture and performance as component of the MPI-Earth System Model in different CMIP5 experimental realizations. *Journal of Advances in Modeling Earth System*, 5, 287-315.
- IPCC. (2014). Climate Change 2014: Impacts, Adaptation, and Vulnerability. Part A: Global and Sectoral Aspects. *Contribution of Working Group II to the Fifth Assessment Report of the Intergovernmental Panel on Climate Change*. Cambridge University Press, Cambridge, United Kingdom and New York, NY, USA, 1132 pp.
- Jessome, A. (1977). Strength and related properties of woods grown in Canada. *Forestry Tech. Report no. 21*. Eastern Forest Products Laboratory. Ottawa, Canada. 37 pp.
- Johansson, P., & Lofgren, K. (1985). *The Economics of Forestry and Natural Resources*. U.K.: Basil Blackwell Ltd.

- Johnston, M., Webber, S., Williamson, T., Hirsch, K., Service, C. F., & Columbia, B. (2009). Climate change impacts and adaptation strategies for the forest sector in Canada. In *2nd Climate Change Technology Conference* (pp. 1–13). Hamilton, ON.
- Johnstone, J., Hollingsworth, T., Chapin, F., & Mack, M. (2010). Changes in fire regime break the legacy lock on successional trajectories in Alaskan boreal forest. *Global Change Biology*, *16*, 1281–1295.
- Jungclaus, J., Fischer, N., Haak, H., Lohmann, K., Marotzke, J., Matei, D., ... von Storch, J. (2013). Characteristics of the ocean simulations in MPIOM, the ocean component of the MPI-Earth System Model. *Journal of Advances in Modeling Earth Systems*, *5*, 422–446.
- Kimball, B. (1975). Carbon dioxide and agricultural yield: An assemblage and analysis of 430 prior observations. *Agronomy Journal*, *75*, 779–788.
- Kirilenko, A., & Sedjo, R. (2007). Climate change impacts on forestry. *Proceedings of the National Academy of Sciences of the United States of America*, *104*(50), 19697–19702. <http://doi.org/10.1073/pnas.0701424104>
- Kula, E., & Gunalay, Y. (2012). Optimum forest rotation with carbon sequestration. *Environmental Impact Assessment Review*, *37*, 18–22.
- Liu, J., Chen, J. M., Cihlar, J., & Chen, W. (2002). Net primary productivity mapped for Canada at 1-km resolution. *Global Ecology and Biogeography*, *11*, 115–129. <http://doi.org/10.1046/j.1466-822X.2002.00278.x>
- Mann, I. K., Wegrzyn, J. L., & Rajora, O. P. (2013). Generation, functional annotation and comparative analysis of black spruce (*Picea mariana*) ESTs: an important conifer genomic resource. *BMC Genomics*, *14*(1), 1. <http://doi.org/10.1186/1471-2164-14-702>
- Masek, J. G., Cohen, W. B., Leckie, D., Wulder, M. A., Vargas, R., De Jong, B., ... Smith, W. B. (2011). Recent rates of forest harvest and conversion in North America. *Journal of Geophysical Research: Biogeosciences*, *116*(2), G00K03. <http://doi.org/10.1029/2010JG001471>
- McGuire, A., Melillo, J., Joyce, L., Kicklighter, D., Grace, A., Moore III, B., & Vorosmarty, C. (1992). Interactions between carbon and nitrogen dynamics in estimating net primary productivity for potential vegetation in North America. *Global Biogeochemical Cycles*, *6*(2), 101–124.
- McGuire, A., Melillo, J., Kicklighter, D., Pan, Y., Xiao, X., et al. (1996). Equilibrium responses of global net primary production and carbon storage to doubled

- atmospheric carbon dioxide: Sensitivity to changes in vegetation nitrogen concentration. *Global Biogeochemical Cycles*, 11, 173-189.
- McKenney, D., Hutchinson, M., Papadopol, P., Lawrence, K., Pedlar, J., Campbell, K., ... Owen, T. (2011). Customized spatial climate models for North America. *Bulletin of American Meteorological Society-BAMS December*, 1611-1622.
- Mckenney, D. W., Pedlar, J. H., Hutchinson, M., Papadopol, P., Lawrence, K., Campbell, K., ... Price, D. (2013). Spatial climate models for Canada's forestry community. *Forestry Chronicle*, 89(5), 659-663.
- McKenney, D. W., Yemshanov, D., Fox, G., & Ramlal, E. (2004). Cost estimates for carbon sequestration from fast growing poplar plantations in Canada. *Forest Policy and Economics*, 6(3-4), 345-358. <http://doi.org/10.1016/j.forpol.2004.03.010>
- Meinshausen, M., Meinshausen, N., Hare, W., Raper, S. C. B., Frieler, K., Knutti, R., ... Allen, M. R. (2009). Greenhouse-gas emission targets for limiting global warming to 2 degrees C. *Nature*, 458(7242), 1158-1162. <http://doi.org/10.1038/nature08017>
- Meinshausen, M., Smith, S. J., Calvin, K., Daniel, J. S., Kainuma, M. L. T., Lamarque, J., ... van Vuuren, D. P. P. (2011). The RCP greenhouse gas concentrations and their extensions from 1765 to 2300. *Climatic Change*, 109(1), 213-241. <http://doi.org/10.1007/s10584-011-0156-z>
- Nozawa, T., Nagashima, T., Ogura, T., Yokohata, T., Okada, N., & Shiogama, H. (2007). *Climate change simulations with a coupled ocean-atmosphere GCM called the Model for Interdisciplinary Research on Climate: MIROC*. Tsukuba, Japan. 1-20.
- OMNR. Annual report on forest management 2012-2013. (2013). *Ontario Ministry of Natural Resources*.
- Parker, W., Nielson, G., Gleeson, J., & Keen, R. (2009). Forecasting carbon storage and carbon offsets for Southern Ontario afforestation projects: The 50 million tree planting program. *Climate Change Research Note*, 10, 1-8.
- Payandeh, B. (1991). Plonski's (metric) yield tables formulated. *The Forestry Chronicle*, 67(5), 545-546.
- Payandeh, B., & Wang, Y. (1996). Variable stocking version of Plonski's yield tables formulated. *The Forestry Chronicle*, 72(2), 181-184.
- Plantinga, A., & Bridsey, R. (1994). Optimal forest stand management when benefits are derived from carbon. *Natural Resource Modelling*, 8(4), 373-387.

- Plonski, W. L. (1956). Normal yield tables for black spruce, jack pine, aspen, and white birch in northern Ontario. *Ontario Department of Lands and Forests*, Toronto, ON., Rep. No. 24, 40.
- Plonski, W. L. (1960). Normal yield tables for Black Spruce, Jack Pine, Aspen, White Birch, tolerant hardwoods, White Pine, and Red Pine for Ontario. *Silvicultural Series Bulletin Ontario Department of Lands and Forests*, 2, 39.
- Pretzsch, H. (2009). *Forest Dynamics, Growth and Yield* (Springer). Berlin.
- Price, D. T., Alfaro, R. I., Brown, K. J., Flannigan, M. D., Fleming, R. A., Hogg, E. H., ... Venier, L. A. (2013). Anticipating the consequences of climate change for Canada's boreal forest ecosystems. *Environmental Review*, 365, 322–365.
- Reick, C., Raddatz, T., Brovkin, V., & Gayler, V. (2013). The representation of natural and anthropogenic land cover change in MPI-ESM. *Journal of Advances in Modeling Earth System*, 5, 1–24.
- Rossi, S., Girard, M.-J., & Morin, H. (2014). Lengthening of the duration of xylogenesis engenders disproportionate increases in xylem production. *Global Change Biology*, 20, 2261–2271.
- Rossi, S., Morin, H., Deslauriers, A., & Plourde, P.-Y. (2011). Predicting xylem phenology in black spruce under climate warming. *Global Change Biology*, 17, 614–625.
- Rossi, S., Morin, H., & Tremblay, M.-J. (2010). Growth and productivity of black spruce (*Picea mariana*) belonging to the first cohort in stands within and north of the commercial forest in Quebec, Canada. *Annals of Forest Science*, 67, 807–807. <http://doi.org/10.1051/forest/2010043>
- Rydge, J. (2015). Implementing Effective Carbon Pricing. *New Climate Economy*, London and Washington, DC. <http://doi.org/http://2015.newclimateeconomy.report/wp-content/uploads/2015/10/Implementing-Effective-Carbon-Pricing.pdf>
- Samuelson, P. (1976). Economics of forestry in an evolving society. *Economic Inquiry*, 14(4), 466–492.
- Sanford, T., Frumhoff, P., Luers, A., & Gullett, J. (2014). The climate policy narrative for a dangerously warming world. *Nature Climate Change*, 4, 164–166.

- Schmidt, G. A., Kelley, M., Nazarenko, L., Ruedy, R., Russell, G. L., et al. (2014). Configuration and assessment of the GISS ModelE2 contributions to the CMIP5 archive. *Journal of Advances in Modeling Earth Systems*, 6(1), 141–184.
- Schmidt, G. A., Ruedy, R., Hansen, J. E., Aleinov, I., Bell, N., Bauer, M., et al. (2006). Present-day atmospheric simulations using GISS Model: Comparison to in situ, satellite, and reanalysis data. *Journal of Climate*, 19(1), 153–192.
- Šeparović, L., Alexandru, A., Laprise, R., Martynov, A., Sushama, L., et al. (2013). Present climate and climate change over North America as simulated by the fifth-generation Canadian regional climate model. *Climate Dynamics*, 41(11), 3167–3201.
- Skidmore, A. (2002). *Environmental modelling with GIS and remote sensing*. New York, NY: Taylor & Francis.
- Stainback, G., & Alavalapati, J. (2AD). Economic analysis of slash pine forest carbon sequestration in the southern U.S. *Journal of Forest Economics*, 8(2), 105–117.
- Stevens, B., Giorgetta, M., Esch, M., Mauritsen, T., Crueger, T., Rast, S., ... Roeckner, E. (2013). Atmospheric component of the MPIM Earth System Model: ECHAM6. *Journal of Advances in Modelling Earth Systems*, 5, 1–27.
- Taylor, K., Stouffer, R., & Meehl, G. (2009). A summary of the CMIP5 experimental design. *WCRP CMIP Rep.* 1-33.
- The State of Canada's Forests. Annual Report 2015. (2015). *Natural Resources Canada, Canadian Forest Service*, 1-63.
- Ueyama, M., Kudo, S., Iwama, C., Nagano, H., Kobayashi, H., Harazono, Y., & Yoshikawa, K. (2015). Does summer warming reduce black spruce productivity in interior Alaska? *Journal of Forest Research*, 20, 52–59.
- Ung, C. H., Bernier, P. Y., Guo, X. J., & Lambert, M. C. (2009). A simple growth and yield model for assessing changes in standing volume across Canada's forests. *Forestry Chronicle*, 85(1), 57–64.
- van Kooten, G. C., Binkley, C. S., & Delcourt, G. (1995). Effect of Carbon Taxes and Subsidies on Optimal Forest Rotation Age and Supply of Carbon Services. *American Journal of Agricultural Economics*, 77(2), 365–374. <http://doi.org/10.2307/1243546>
- van Kooten, G. C., Krcmar-Nozic, E., Stennes, B., & van Gorkom, R. (1999). Economics of fossil fuel substitution and wood product sinks when trees are planted to sequester carbon on agricultural lands in western Canada. *Canadian Journal of Forest Research*, 29(11), 1669–1678. <http://doi.org/10.1139/x99-145>

- Waring, R., & Running, S. (2007). *Forest Ecosystems: Analysis at multiple scales* (3rd ed.). San Diego, California: Elsevier.
- Watanabe, S., Hajima, T., Sudo, K., Nagashima, T., Takemura, T., Okajima, H., ... Kawamiya, M. (2011). MIROC-ESM: model description and basic results of CMIP5-20c3m experiments. *Geoscientific Model Development Discussions*, 4(2), 1063–1128. <http://doi.org/10.5194/gmdd-4-1063-2011>
- Way, D., & Sage, R. (2008). Thermal acclimation of photosynthesis in black spruce [*Picea mariana* (Mill.) B.S.P.]. *Plant, Cell & Environment*, 31, 1250–1262.
- Wayne, G. (2013). *The beginner's guide to Representative Concentration Pathways*.
- World Bank. (2014). *World Bank Group: Climate Change*. Retrieved from http://www.csmenergy.com.au/carbon_price.html
- Xiao, X., Melillo, J. M., Kicklighter, D. W., Mcguire, A. D., Stone, P. H., & Sokolov, A. P. (1996). Relative Roles of Changes in CO₂ and Climate to Equilibrium Responses of Net Primary Production and Carbon Storage of the Terrestrial Biosphere. *Global Change Biology*, (508), 1–32.
- Yang, J., McKenney, D. W., & Weersink, A. (2015). Should climate change make us think more about the economics of forest management?. *The Forestry Chronicle*, 91(1), 23-31.
- Yemshanov, D., McKenney, D., Fraleigh, S., & D'Eon, S. (2007). An integrated spatial assessment of the investment potential of three species in southern Ontario, Canada inclusive of carbon benefits. *Forest Policy and Economics*, 10(1-2), 48–59. <http://doi.org/10.1016/j.forpol.2007.03.001>
- Yemshanov, D., McKenney, D. W., Hatton, T., & Fox, G. (2005). Investment Attractiveness of Afforestation in Canada Inclusive of Carbon Sequestration Benefits. *Canadian Journal of Agricultural Economics/Revue Canadienne D'agroéconomie*, 53(4), 307–323. <http://doi.org/10.1111/j.1744-7976.2005.00021.x>
- Zhang, K., Kimball, J., Hogg, E., Zhao, M., Oechel, W., Cassano, J., & Running, S. (2008). Satellite-based model detection of recent climate-driven changes in northern high-latitude vegetation productivity. *Journal of Geophysical Research Biogeosciences*, 113, 1-13.
- Zhu, L., & Southworth, J. (2013). Disentangling the relationships between Net primary production and precipitation in Southern Africa savannas using satellite observations

from 1982 to 2010. *Remote Sensing*, 5(8), 3803–3825.
<http://doi.org/10.3390/rs5083803>

FIGURES

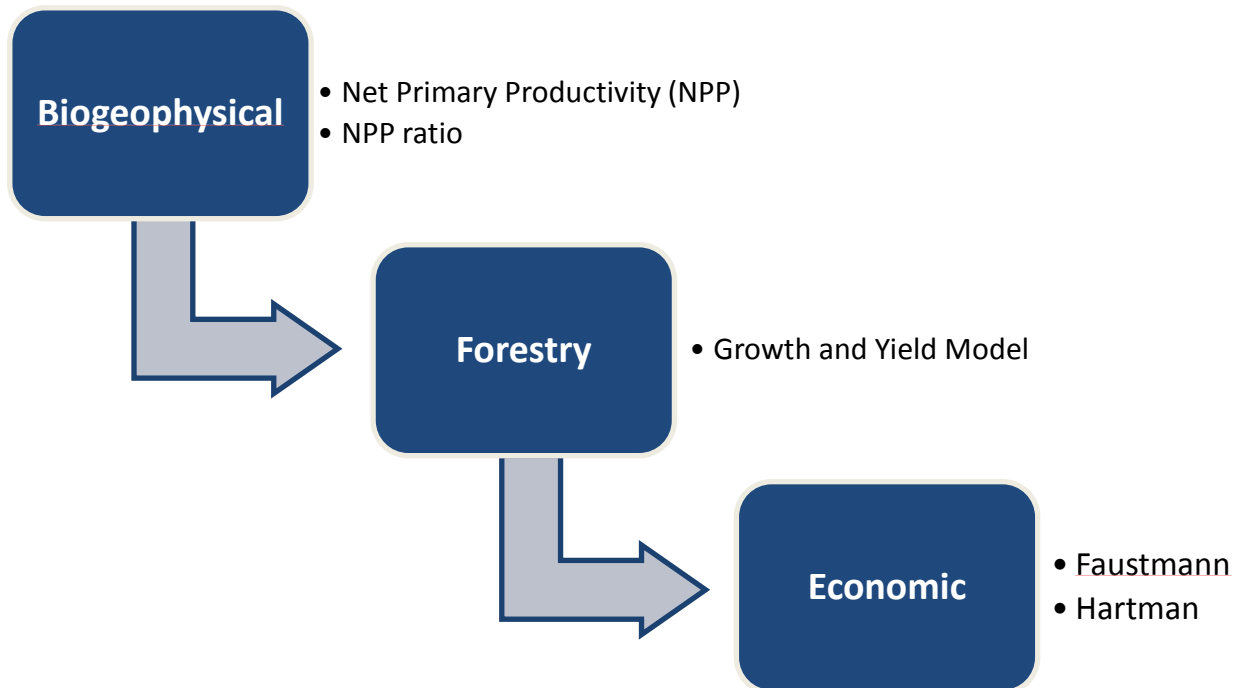


Figure 1. Overview of study methodology including the integration of biogeophysical, forest growth and yield, and economic models to project future timber growth and present value estimates. We used temporal and spatial distributions of GCM-simulated NPP to modify gross merchantable volume trajectories obtained from the black spruce growth and yield model. Then, net present values were calculated with and without carbon sequestration benefits to represent the economic feasibility of the silvicultural investment using Hartman and Faustmann economic models, respectively.

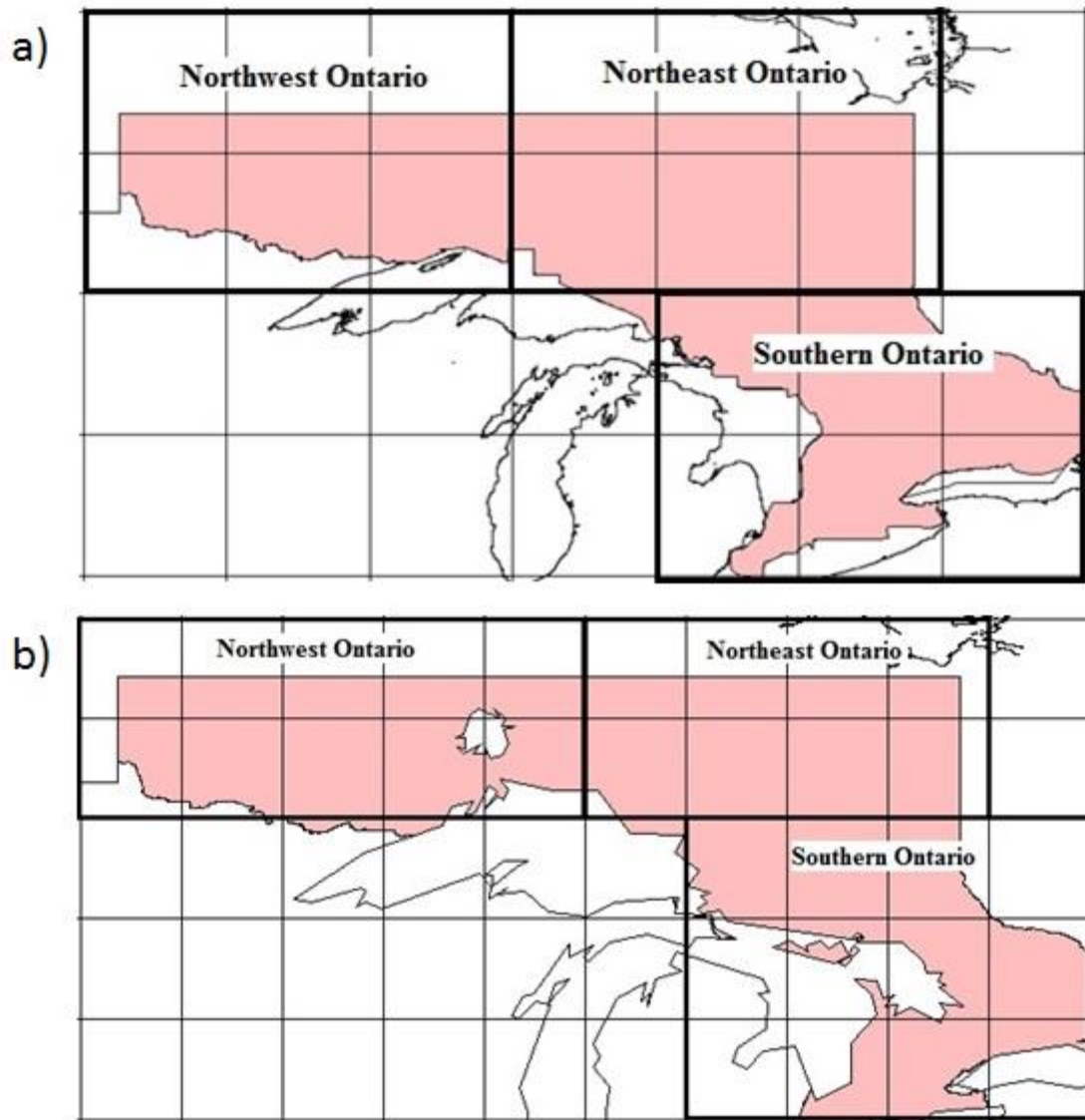


Figure 2. Study area, focused on the province of Ontario in Canada below 52° latitude. Model grids are based on the resolutions of global climate model, GCMs (a) CanESM2 and MIROC (~2.8°) and (b) MPI (~2.5°). Study area has been divided into three regions – northwest, northeast, and southern Ontario. (a) For CanESM2 and MIROC, -87.4 decimal degrees longitude is used for a division between NW and NE Ontario and 47.4 decimal degrees latitude is used for a division between northern and southern Ontario. (b) For MPI, -86.4 decimal degrees longitude is used for a division between NW and NE Ontario and 48.4 decimal degrees latitude is used for a division between northern and southern Ontario. Note: Forest growth and yield tables are not applicable over 52° latitude.

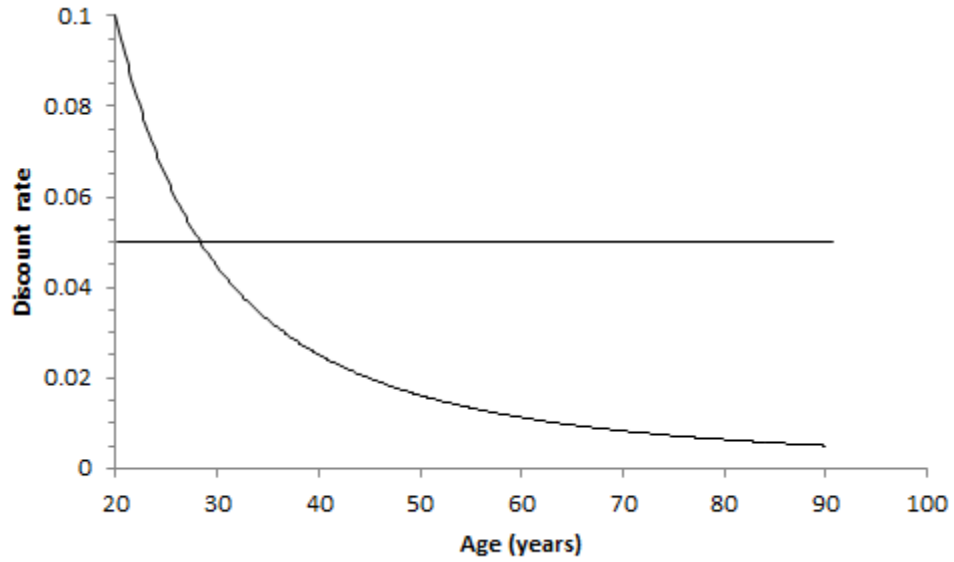


Figure 3. First order condition for optimization for harvest age. The curve line is the relative value growth rate. The horizontal line represents a discount rate of 5%. The intersection of the two represents the optimal harvest age, 29.3 years, in this example.

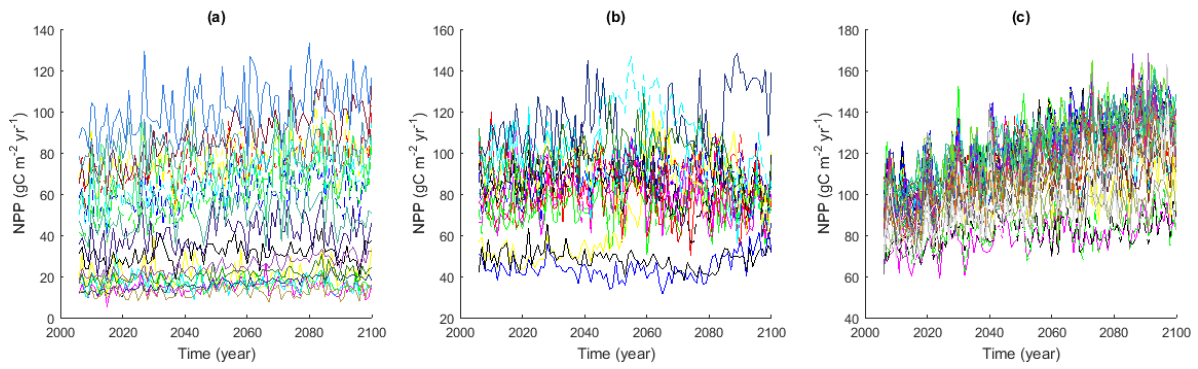


Figure 4. Time series of grid-level simulated Net Primary Production (NPP) from three global climate models – (a) CanESM2 (Canadian), (b) MIROC (Japanese), and (c) MPI (European) for IPCC-RCP 8.5 future climate scenario. Each line represents a grid-specific NPP estimate from 2006 to 2100.

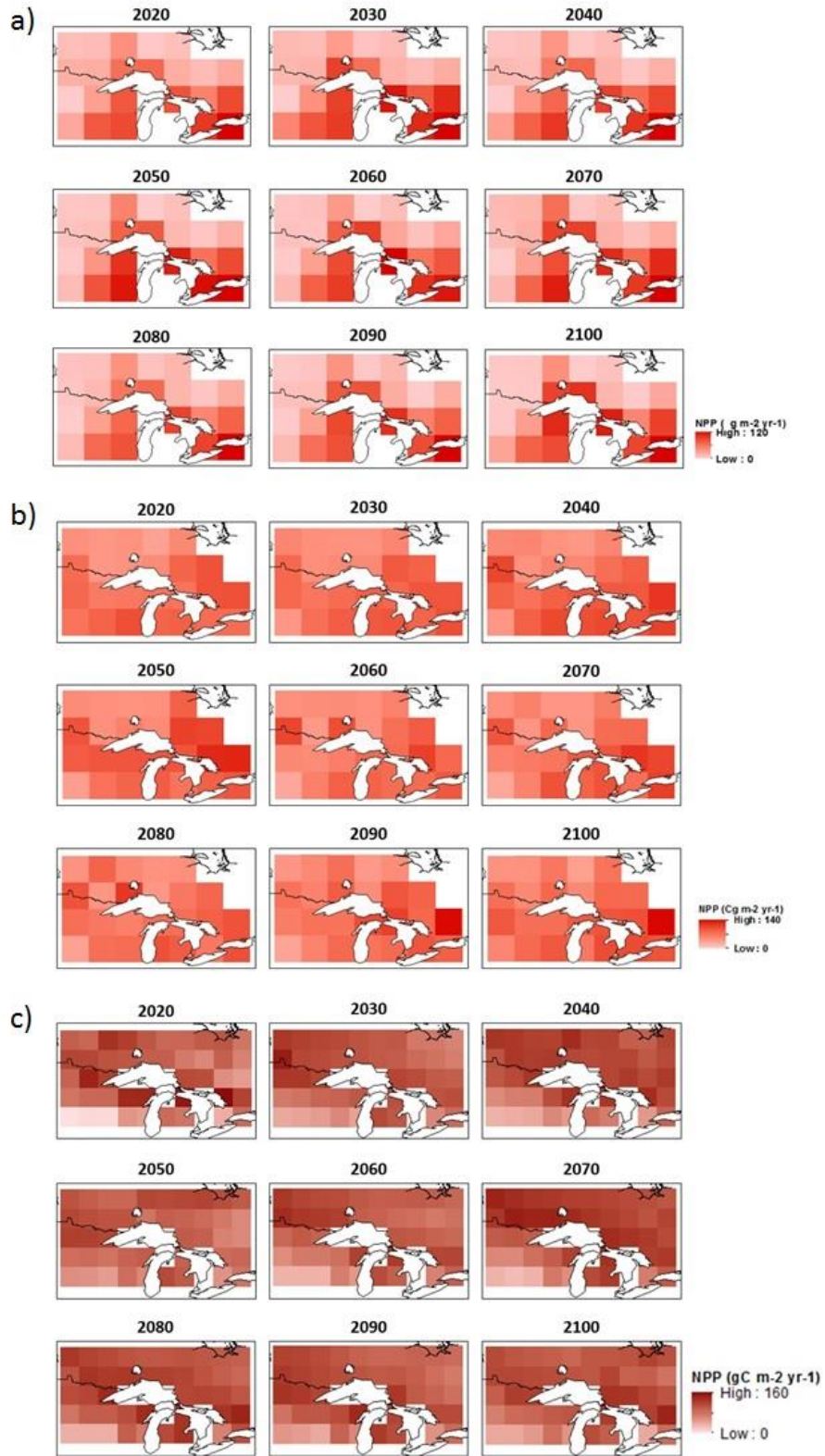


Figure 5. Spatial distribution of annual Net Primary Production (NPP) change over time in the study area as simulated by (a) CanESM2, (b) MIROC, and (c) MPI models.

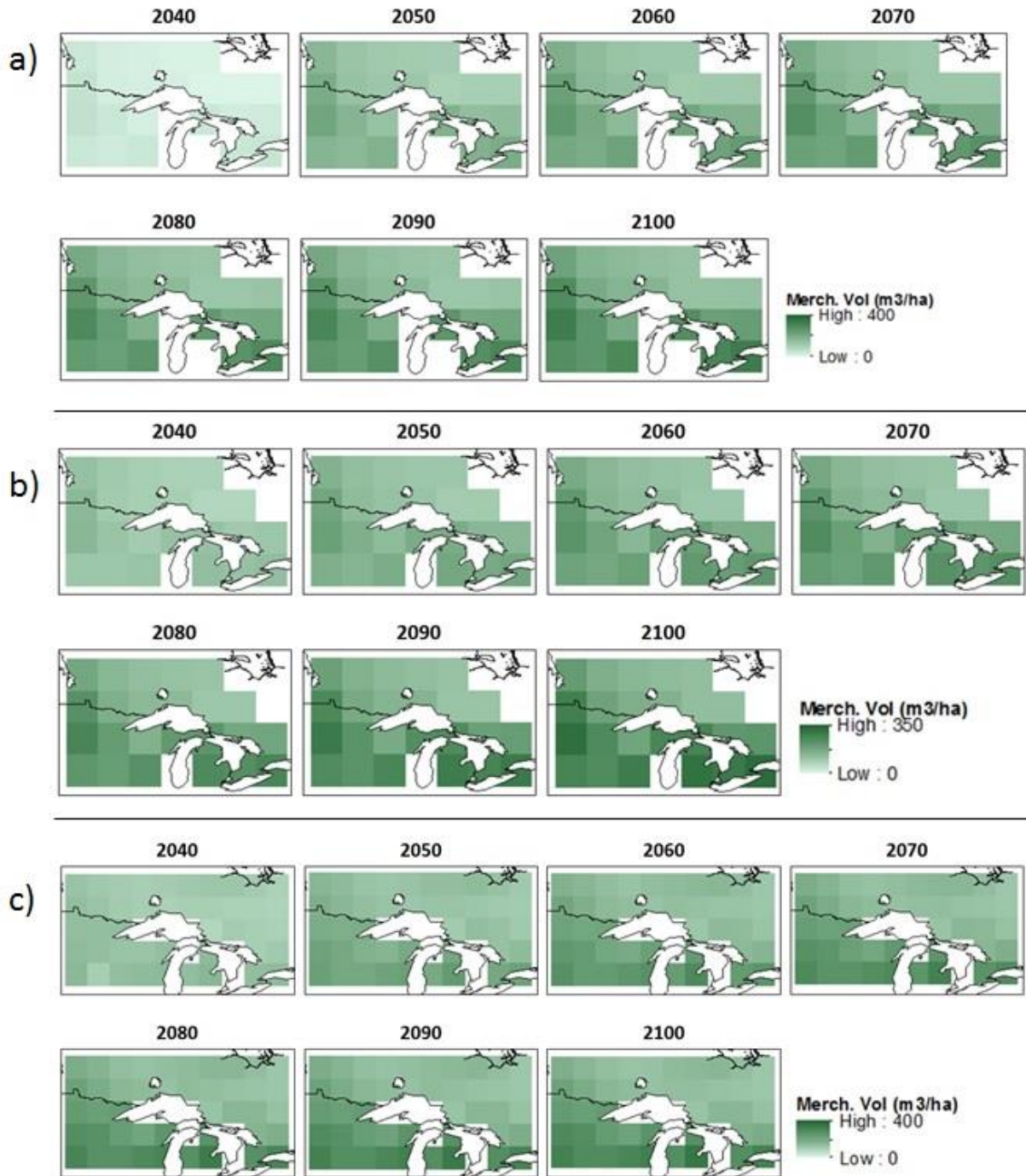


Figure 6. Spatial distribution of gross merchantable wood volume ($\text{m}^3 \text{ha}^{-1}$) of black spruce over the study period based on (a) CanESM2-, (b) MIROC-, and (c) MPI model simulated annual Net Ecosystem Productivity (NPP) ratio, and temperature and precipitation-specific grid conditions.

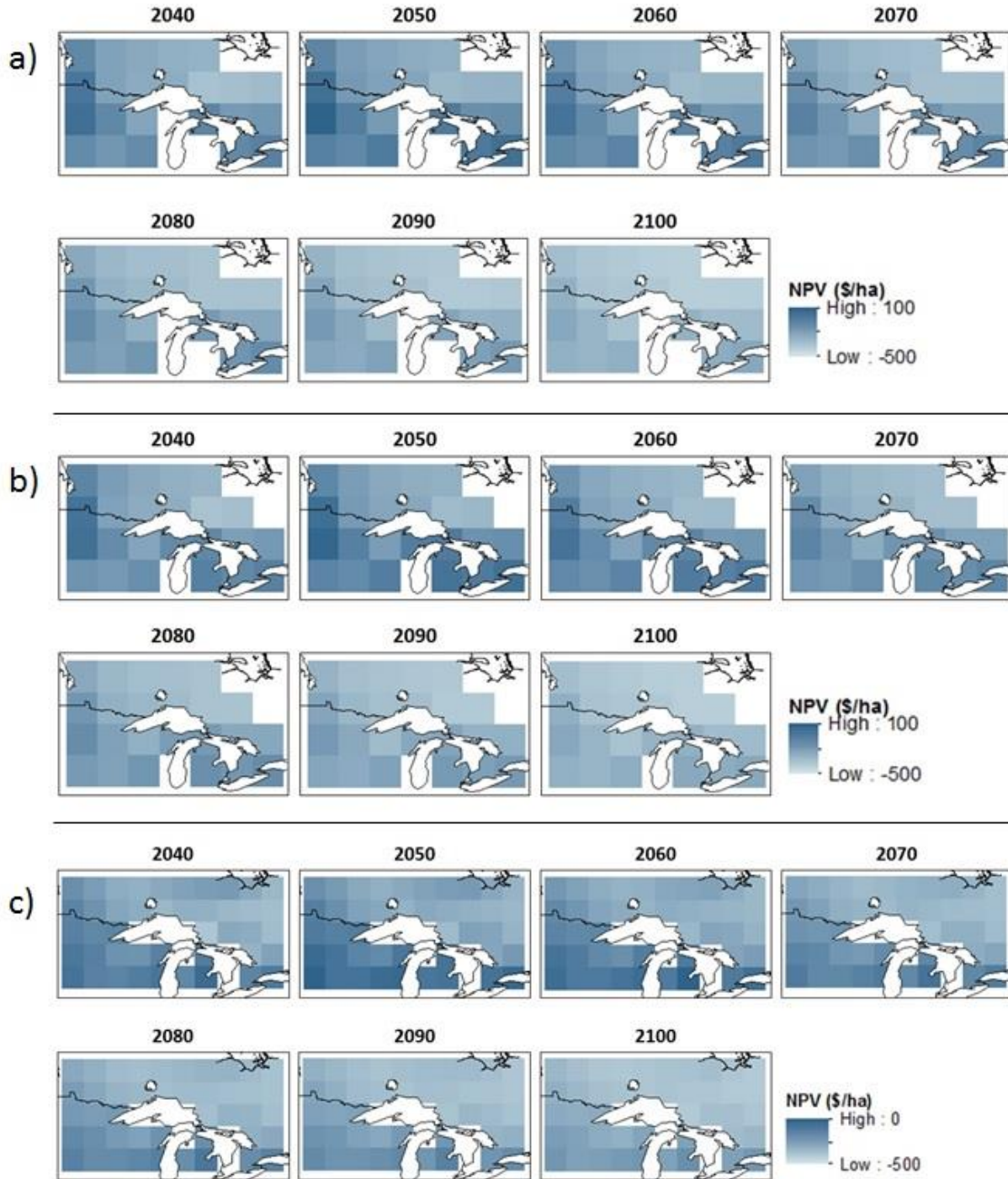


Figure 7. Spatial distribution of NPVs of black spruce exclusive carbon sequestration benefits in the study area using Faustmann model based on (a) CanESM2, (b) MIROC, and (c) MPI models.

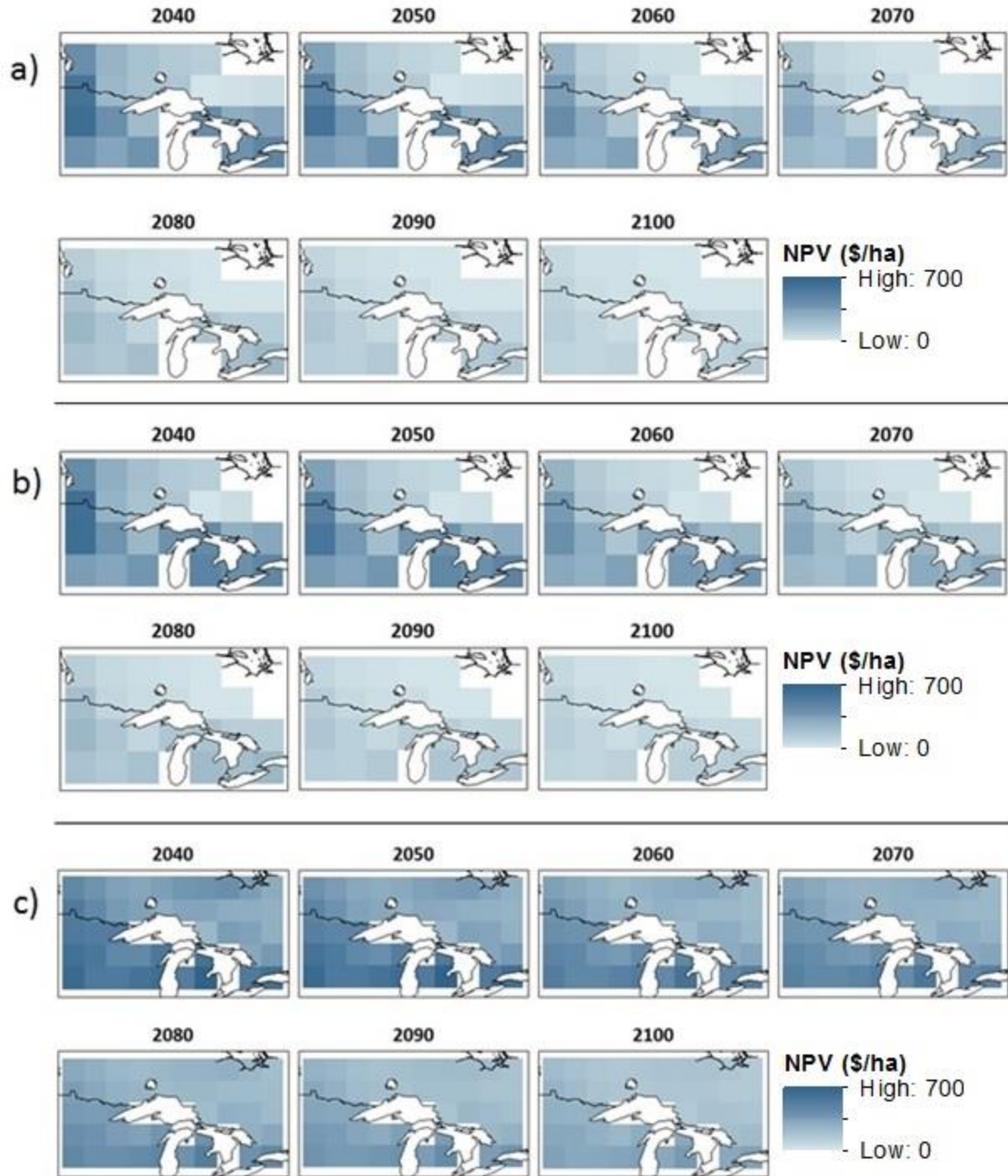


Figure 8. Spatial distribution of NPVs of black spruce inclusive of carbon sequestration benefits in the study area using a modified Hartman model based on (a) CanEMS2, (b) MIROC, and (c) MPI model.

Table 1: General assumptions and data used in baseline scenarios and sensitivity analyses

Parameters and assumptions	Value
Discount rate (%)	4, (2, 8)*
Establishment costs (\$ ha ⁻¹)	500, (200, 1000)*
Timber price (\$ m ⁻³)	20, (50)*
Price for carbon (\$ ton ⁻¹ CO ₂)	5, (10, 20)* – only for a modified Hartman

* Values in parentheses represent sensitivity analyses values

Table 2: Summary table of Net Present Values (NPVs) of timber and carbon by regions

Model	Scenario	OHA*	Northwest Ontario				Northeast Ontario				Southern Ontario			
			Mean	Max.	Min.	Std.	Mean	Max.	Min.	Std.	Mean	Max.	Min.	Std.
Can-ESM2	W*	2049	-136	33	-221	99	-265	-220	-300	33	-51	29	-128	67
	W+C*	2052	430	503	345	100	305	347	272	31	522	607	445	70
MIROC	W	2048	-137	38	-228	103	-269	-226	-307	33	-39	18	-130	68
	W+C	2054	424	592	337	96	304	345	274	29	471	600	443	68
MPI	W	2048	-226	-105	-297	61	-263	-208	-330	39	-90	57	-258	120
	W+C	2052	341	459	282	60	306	353	248	35	485	628	321	118

*OHA represents optimum harvest age; W represents wood only scenario; W+C represents both wood and carbon value scenario

Table 3: Sensitivity analyses of wood-only scenario (Faustmann model). Optimal net present value with varying discount rate, establishment costs, and stumpage value.

	CanESM2			MIROC			MPI					
Scenarios	r = 2% (46)	r = 4% (39)	r = 8% (33)	r = 2% (45)	r = 4% (38)	r = 8% (33)	r = 2% (46)	r = 4% (38)	r = 8% (32)			
NW	666	-136	-430	661	-137	-424	391	-226	-444			
NE	267	-265	-456	261	-269	-454	277	-263	-453			
S	1012	-51	-416	1047	-39	-409	900	-90	-419			
Scenarios	C = \$200 (35)	C = \$500 (39)	C = \$1000 (46)	C = \$200 (36)	C = \$500 (38)	C = \$1000 (45)	C = \$200 (36)	C = \$500 (38)	C = \$1000 (46)			
NW	262	-136	-762	257	-137	-759	-132	-226	-841			
NE	125	-265	-876	122	-269	-876	-171	-263	-873			
S	332	-51	-663	346	-39	-653	-2	-90	-696			
Scenarios	P = \$20 (39)		P = \$50 (34)		P = \$20 (38)		P = \$50 (36)		P = \$20 (38)		P = \$50 (36)	
NW	-136		660		-137		643		-226		418	
NE	-265		316		-269		306		-263		322	
S	-51		824		-39		864		-90		744	

*Values in parentheses represent optimal harvest age

Table 4: Sensitivity analyses of wood + carbon scenario (modified Hartman model). Optimal net present value with varying discount rate, establishment costs, stumpage value, and carbon price when the carbon uptake value is considered.

	CanESM2			MIROC			MPI					
Scenarios	r = 2% (49)	r = 4% (42)	r = 8% (35)	r = 2% (47)	r = 4% (44)	r = 8% (35)	r = 2% (49)	r = 4% (42)	r = 8% (35)			
NW	1276	430	108	1285	424	109	1000	341	90			
NE	880	305	81	880	304	81	887	306	82			
S	1631	522	122	1662	529	125	1518	485	115			
Scenarios	C = \$200 (39)	C = \$500 (42)	C = \$1000 (49)	C = \$200 (38)	C = \$500 (44)	C = \$1000 (49)	C = \$200 (38)	C = \$500 (42)	C = \$1000 (51)			
NW	811	430	-177	812	424	-175	723	341	-251			
NE	682	305	-285	679	304	-286	686	306	-280			
S	896	522	-80	909	529	-68	858	485	-111			
Scenarios	P = \$20 (42)		P = \$50 (38)		P = \$20 (44)		P = \$50 (35)		P = \$20 (42)		P = \$50 (36)	
NW	430		1184		424		1216		341		978	
NE	305		851		304		871		306		882	
S	522		1391		529		1424		485		1304	
Scenarios	P _{cs} = \$5 (42)	P _{cs} = \$10 (42)	P _{cs} = \$20 (51)	P _{cs} = \$5 (44)	P _{cs} = \$10 (45)	P _{cs} = \$20 (56)	P _{cs} = \$5 (42)	P _{cs} = \$10 (46)	P _{cs} = \$20 (60)			
NW	430	504	675	424	502	680	341	420	624			
NE	305	379	573	304	384	589	306	387	601			
S	522	596	773	529	608	783	485	565	745			

*Values in parentheses represent optimal harvest age

APPENDIX

Data downloading and analyzing for CanESM2

```

close all;
clear all;
clc;

%fetch land mask
pth = sprintf('/Users/User/Downloads/Suo_Data/BG1_2_con/');

%fetch model output
infile_can=[pth 'npp_Lmon_CanESM2_historical_rlilp1_185001-%year%.nc'];
infile_ca85=[pth 'npp_Lmon_CanESM2_rcp85_rlilp1_200601-%year%.nc'];

for hyear=200512;
    ind=find(hyear==200512);
    ind=((ind-1).*12)+[1:12];

    infileHI=strrep(infile_can, '%year%', num2str(hyear));

    NPP_his_can=ncread(infileHI, 'npp');

    NPP_his_can=squeeze(NPP_his_can);
end

for cyear=2100; %year loop
    ind=find(cyear==2100);
    ind=((ind-1).*12)+[1:12];

    infile8= strrep(infile_ca85, '%year%', num2str(cyear));

    NPP85_can=ncread(infile8, 'npp'); %swap out whatever field you are
interested in here

    NPP85_can=squeeze(NPP85_can);
end

NPP_his_can=permute(NPP_his_can,[2 1 3]); %historical data
NPP85_can=permute(NPP85_can,[2 1 3]); %future data

adj=60*60*24*(365/12)*1000; %unit conversion for carbon fluxes: kgC/m2/s ->
gC/m2/mon

NPP_his_can=NPP_his_can.*adj;
NPP85_can=NPP85_can.*adj;

NPP_his_can=single(NPP_his_can);
NPP85_can=single(NPP85_can);

NPP_his_can(NPP_his_can < 0.001) = NaN;
NPP85_can(NPP85_can < 0.001) = NaN;

```

```

NPP_his_can = rot90(NPP_his_can);
NPP_his_can = rot90(NPP_his_can);
NPP_his_can = fliplr(NPP_his_can);

NPP85_can = rot90(NPP85_can);
NPP85_can = rot90(NPP85_can);
NPP85_can = fliplr(NPP85_can);

NPP_his_can = NPP_his_can(13:16,95:101,1513:1872); %30year baseline for
CanESM
NPP85_can = NPP85_can(13:16,95:101,1:1140);

load('canesm2_nppratio.mat'); %load canesm2-calculated npp ratio

t = [1:91]; %set age (1 to 91 years)
t = t';

%black spruce parameters
bs10=6.2061;
bs11=0.1397;
bs12=-0.0012;
bs20=-49.0695;
bs21=-2.4537;
bs22=0;
bsCd=1.1537;

% obtaining/analyzing mean annual temperature and precipitation 1961-1990

pth = sprintf('/Users/User/Downloads/Suo_Data/BG1_2_con/MAT_PREC/');
out = [pth 'out%year%.txt'];

for j = 1961:1990

    out = strrep(out, '%year%', num2str(j));
    his{j-1961+1} = load(out);

    map{j-1961+1} = his{1,j-1961+1}(2:end,14); %mean annual precipitation

    mapa{j-1961+1} = map{j-1961+1}(1:5); %divide the array to put NaN
(waterbody)
    mapa{j-1961+1} = [mapa{j-1961+1};NaN]; %add NaN to waterbody location
    mapb{j-1961+1} = map{j-1961+1}(6:27);
    map{j-1961+1} = [mapa{j-1961+1};mapb{j-1961+1}]; %join together
    map{j-1961+1} = reshape(map{j-1961+1},[7,4]); %reshape
    map{j-1961+1} = map{j-1961+1}.'; %switch row and col

    mat_h{j-1961+1} = his{1,j-1961+1}(2:end,28); %annual mean temperature

    mata{j-1961+1} = mat_h{j-1961+1}(1:5);
    mata{j-1961+1} = [mata{j-1961+1};NaN];
    matb{j-1961+1} = mat_h{j-1961+1}(6:27);
    mat_h{j-1961+1} = [mata{j-1961+1};matb{j-1961+1}];

```

```

mat_h{j-1961+1} = reshape(mat_h{j-1961+1}, [7,4]);
mat_h{j-1961+1} = mat_h{j-1961+1}.';

vbs_his{j-1961+1} = exp(bs10+bs11.*mat_h{1,j-1961+1}+bs12.*map{1,j-
1961+1}+(bs20+bs21.*mat_h{1,j-1961+1}+bs22.*map{1,j-1961+1}))/ (j-
1961+1)).*bsCd;

end

vbs_avg =
(vbs_his{1,1}+vbs_his{1,2}+vbs_his{1,3}+vbs_his{1,4}+vbs_his{1,5}+vbs_his{1,6}
+vbs_his{1,7}+vbs_his{1,8}+vbs_his{1,9}+vbs_his{1,10}+vbs_his{1,11}+vbs_his{
1,12}+vbs_his{1,13}+vbs_his{1,14}+vbs_his{1,15}+vbs_his{1,16}+vbs_his{1,17}+v
bs_his{1,18}+vbs_his{1,19}+vbs_his{1,20}+vbs_his{1,21}+vbs_his{1,22}+vbs_his{
1,23}+vbs_his{1,24}+vbs_his{1,25}+vbs_his{1,26}+vbs_his{1,27}+vbs_his{1,28}+v
bs_his{1,29}+vbs_his{1,30})/30;

map30 = [420 568 623 666 686 NaN 676; 472 713 741 781 924 881 858; 538 656
786 701 670 809 759; 792 856 839 94 781 816 805]; %30-year mean annual
precipitation
mat30 = [0.52 -0.03 -0.52 -0.67 -0.91 NaN -1.18;3.48 2.71 1.57 1.95 1.41 1
1.03; 5.42 4.54 3.41 5.41 5.31 4.96 4.64;6.65 6.67 7.71 7.86 7.8 7.65
8.41]; %30-year annual mean temperature

%calculate gross merch volume using Ung et al. equation
for k = 2010:2100

vbs{k-
2010+1}=exp(bs10+bs11.*mat30+bs12.*map30+(bs20+bs21.*mat30+bs22.*map30))/ (k-
2010+1)).*bsCd;

end

%adjust equation so it accumulates growth properly over time
for k = 2011:2100

vbs_cal{k-2011+1} = ((vbs{k-2010+1}-vbs{k-2011+1})).*rtNPP{k-
2010+1})+vbs{k-2011+1};

end

%% Faustmann model (timber only)

r2 = 1.020201; %discount rate=2%
r4 = 1.040811; %discount rate=4%
r8 = 1.083287; %discount rate=8%
P = 20; %stumpage value = $20/m3
P5 = 50; %SA stumpage value = $50/m3
C = 500; %establishment cost = $500/ha
C2 = 200; %sensitivity analysis C = $200/ha
C10 = 1000; %sensitivty analysis C = $1000/ha

array = [1 1 1 1 1 NaN 1; 1 1 1 1 1 1 1; 1 1 1 1 1 1 1 ; 1 1 1 1 1 1 1 ];

```

```

% NPV using a Faustmann model
for a = 0:89

    NPVf{a+1} = (((P.*vbs_cal{a+1})-C).*exp(-0.04.*(a+1))./(1-(exp(-
0.04.*(a+1)))))-500; %baseline
    NPVf_r2{a+1}=(((P.*vbs_cal{a+1})-C).*exp(-0.02.*(a+1))./(1-(exp(-
0.02.*(a+1)))))-500; %discount rate = 2%
    NPVf_r8{a+1}=(((P.*vbs_cal{a+1})-C).*exp(-0.08.*(a+1))./(1-(exp(-
0.08.*(a+1)))))-500; %discount rate = 8%
    NPVf_c2{a+1}=(((P.*vbs_cal{a+1})-C2).*exp(-0.04.*(a+1))./(1-(exp(-
0.04.*(a+1)))))-C2; %establishment cost = $200
    NPVf_c10{a+1}=(((P.*vbs_cal{a+1})-C10).*exp(-0.04.*(a+1))./(1-(exp(-
0.04.*(a+1)))))-C10; %establishment cost = $1000
    NPVf_p5{a+1}=(((P5.*vbs_cal{a+1})-C).*exp(-0.04.*(a+1))./(1-(exp(-
0.04.*(a+1)))))-500; %stumpage value = $50

end

%% Hartman model (wood + carbon)

% wood + carbon
cs5 = 5; % carbon price = $5
cs10 = 10; % carbon price = $10
cs20 = 20; % carbon price = $20
qc = 0.3; %conversion factor from biomass volume to carbon

% following represents carbon pricing model
fun1 = @(x) exp(-0.04.*x).*5.*(13.2649.*exp(-0.0253.*x)).*(1-exp(-
0.0253.*x)).^1.64);
fun0 = @(x) exp(-0.04.*x).*(13.2649.*exp(-0.0253.*x)).*(1-exp(-
0.0253.*x)).^1.64);
fun2 = @(x) exp(-0.04.*x).*(13.2649.*exp(-0.0253.*x)).*(1-exp(-
0.0253.*x)).^1.64);
fun3 = @(x) exp(-0.04.*x).*(13.2649.*exp(-0.0253.*x)).*(1-exp(-
0.0253.*x)).^1.64);
fun4 = @(x) exp(-0.08.*x).*(13.2649.*exp(-0.0253.*x)).*(1-exp(-
0.0253.*x)).^1.64);
fun5 = @(x) exp(-0.02.*x).*(13.2649.*exp(-0.0253.*x)).*(1-exp(-
0.0253.*x)).^1.64);

% NPV using a modified Hartman model
for a = 0:89

    NPV_c{a+1}= (((((P.*vbs_cal{a+1})-C).*exp(-
0.04.*(a+1)))+5.*(integral(fun0,0,a+1))-5.*exp(-0.04.*(a+1)).*(198.6.*((1-
exp(-0.0253.*(a+1))).^2.64)))./(1-(exp(-0.04.*(a+1)))))-500; %baseline
    NPV_c10{a+1} = (((((P.*vbs_cal{a+1})-C).*exp(-
0.04.*(a+1)))+10.*(integral(fun2,0,a+1))-10.*exp(-0.04.*(a+1)).*(198.6.*((1-
exp(-0.0253.*(a+1))).^2.64)))./(1-(exp(-0.04.*(a+1)))))-500;
    NPV_c20{a+1} = (((((P.*vbs_cal{a+1})-C).*exp(-
0.04.*(a+1)))+20.*(integral(fun3,0,a+1))-20.*exp(-0.04.*(a+1)).*(198.6.*((1-
exp(-0.0253.*(a+1))).^2.64)))./(1-(exp(-0.04.*(a+1)))))-500;

```

```
NPV_cp5{a+1} = (((((P5.*vbs_cal{a+1})-C).*exp(-
0.04.*(a+1))+5.*(integral(fun0,0,a+1))-5.*exp(-0.04.*(a+1)).*(198.6.*(1-
exp(-0.0253.*(a+1))).^2.64)))./(1-(exp(-0.04.*(a+1)))))-500;
```

```
NPV_cr2{a+1} = (((((P.*vbs_cal{a+1})-C).*exp(-
0.02.*(a+1))+5.*(integral(fun5,0,a+1))-5.*exp(-0.02.*(a+1)).*(198.6.*(1-
exp(-0.0253.*(a+1))).^2.64)))./(1-(exp(-0.02.*(a+1)))))-500;
```

```
NPV_cr8{a+1} = (((((P.*vbs_cal{a+1})-C).*exp(-
0.08.*(a+1))+5.*(integral(fun4,0,a+1))-5.*exp(-0.08.*(a+1)).*(198.6.*(1-
exp(-0.0253.*(a+1))).^2.64)))./(1-(exp(-0.08.*(a+1)))))-500;
```

```
NPV_cC2{a+1} = (((((P.*vbs_cal{a+1})-C2).*exp(-
0.04.*(a+1))+5.*(integral(fun0,0,a+1))-5.*exp(-0.04.*(a+1)).*(198.6.*(1-
exp(-0.0253.*(a+1))).^2.64)))./(1-(exp(-0.04.*(a+1)))))-500;
```

```
NPV_cC10{a+1}= (((((P.*vbs_cal{a+1})-C10).*exp(-
0.04.*(a+1))+5.*(integral(fun0,0,a+1))-5.*exp(-0.04.*(a+1)).*(198.6.*(1-
exp(-0.0253.*(a+1))).^2.64)))./(1-(exp(-0.04.*(a+1)))))-500;
```

end